



**HAL**  
open science

## A Three-player Nash game for point-wise source identification in Cauchy-Stokes problems

Marwa Ouni, Abderrahmane Habbal, Moez Kallel

► **To cite this version:**

Marwa Ouni, Abderrahmane Habbal, Moez Kallel. A Three-player Nash game for point-wise source identification in Cauchy-Stokes problems. *Journal of Computational and Applied Mathematics*, 2023, 417, pp.23. 10.1016/j.cam.2022.114613 . hal-03523088v2

**HAL Id: hal-03523088**

**<https://inria.hal.science/hal-03523088v2>**

Submitted on 13 Jan 2023

**HAL** is a multi-disciplinary open access archive for the deposit and dissemination of scientific research documents, whether they are published or not. The documents may come from teaching and research institutions in France or abroad, or from public or private research centers.

L'archive ouverte pluridisciplinaire **HAL**, est destinée au dépôt et à la diffusion de documents scientifiques de niveau recherche, publiés ou non, émanant des établissements d'enseignement et de recherche français ou étrangers, des laboratoires publics ou privés.

# A Three-player Nash game for point-wise source identification in Cauchy-Stokes problems

Marwa OUNI<sup>a,c,\*</sup>, Abderrahmane HABBAL<sup>a,b</sup>, Moez KALLEL<sup>c</sup>

<sup>a</sup> *Université Côte d'Azur, Inria, CNRS, LJAD, UMR 7351, Parc Valrose 06108 NICE CEDEX 2, France*

<sup>b</sup> *Polytechnic Mohammed VI University, Benguerir, Morocco*

<sup>c</sup> *University of Tunis El Manar, ENIT-LAMSIN, BP 37, 1002 Tunis-Belvédère, Tunisia*

---

## Abstract

We consider linear steady Stokes flow under the action of a finite number of particles located inside the flow domain. The particles exert point-wise forces on the fluid, and are unknown in number, location and magnitude. We are interested in the determination of these point-wise forces, using only a single pair of partially available Cauchy boundary measurements. The inverse problem then couples two harsh problems : identification of point-wise sources and recovery of missing boundary data. We reformulate it as a three-player Nash game. The first two players aim at recovering the Dirichlet and Neumann missing data, while the third one aims at the point-forces reconstruction of the number, location and magnitude of the point-forces. To illustrate the efficiency and robustness of the proposed algorithm, we finally present several numerical experiments for different geometries and source distribution, including the case of noisy measurements.

*Keywords:* Data completion, Point-force detection, Topological sensitivity, Nash game

---

## 1. Introduction

Detection of point-wise sources in many physical, geophysical and biological processes, is of utmost importance. See e.g. [4] for the detection of pollutant sources, and [21] for detecting radiation sources. For many technological reasons, very often the boundary measurements can be performed only on accessible parts of the whole boundary. Partial availability of boundary data leads to an additional inverse problem formulation, known as Cauchy problem and which has been shown [19] to be ill posed. Our aim here is to develop novel approaches where the two identification problems (sources and missing boundary data) can be handled jointly.

Consider a bounded open domain  $\Omega \subset \mathbb{R}^d$  ( $d=2, 3$ ) occupied by an incompressible viscous fluid, with a smooth enough boundary  $\partial\Omega$ . We assume that the fluid flow is under the action of a finite number of point-wise forces  $F$  located inside  $\Omega$ .

The source term  $F$  is assumed to be a linear combination of Dirac distributions accounting for the collection of the point-wise forces:

$$F = \sum_{k=1}^m \lambda_k \delta_{P_k}, \quad (1)$$

where  $m$  is the total number of point-wise forces,  $\delta_{P_k}$  denotes the classical Dirac distribution with origin the point  $P_k$ , and  $\lambda_k \in \mathbb{R}^d$  is a constant vector. The parameters  $P_k$  and  $\lambda_k$  stand respectively for the position and the magnitude of the  $k$ th point-wise force.

---

\*Corresponding author

*Email addresses:* marwa1ouni@gmail.com (Marwa OUNI), habbal@unice.fr (Abderrahmane HABBAL), moez.kallel@enit.utm.tn (Moez KALLEL)

In this work, we assume that the vectors  $\lambda_k$  are nonzero and that the positions  $P_k$  are well separated and satisfy the following :

$$P_k \neq P_{k'}, \forall k \neq k' \text{ and } \lambda_k \neq 0 \forall k, k' \in \{1, \dots, m\},$$

$$\text{dist}(P_k, \partial\Omega) \geq d_0 > 0, \forall k \in \{1, \dots, m\}. \quad (2)$$

The Cauchy-Stokes inverse problem consists then in a coupled inverse problem : identification of point-wise sources, and recovery of missing boundary data.

The first inverse problem is a classical point-wise source reconstruction. Namely, from given velocity  $G$  and fluid stress forces  $\Phi$  prescribed on  $\Gamma_c$ , where  $\Gamma_c$  is a part of the boundary  $\partial\Omega$ , one has to identify the unknown source-term  $F^*$ , that is, to find the number, the location and the magnitude of these point-wise forces such that the fluid velocity  $u$  and the pressure  $p$  are solution of the following Stokes problem:

$$(\mathcal{CS}) \begin{cases} -\text{div}(\sigma(u, p)) &= F^* & \text{in } \Omega, \\ \text{div} u &= 0 & \text{in } \Omega, \\ u &= G & \text{on } \Gamma_c, \\ \sigma(u, p)n &= \Phi & \text{on } \Gamma_c, \end{cases}$$

where  $n$  is the unit outward normal vector on the boundary, and  $\sigma(u, p)$  the fluid stress tensor defined as follows:

$$\sigma(u, p) = -pI_d + 2\nu D(u)$$

with  $D(u) = \frac{1}{2}(\nabla u + \nabla u^T)$  being the linear strain tensor,  $I_d$  denotes the  $d \times d$  identity matrix and  $\nu > 0$  is a viscosity coefficient that remains constant for all values of applied shear stress. For simplicity and without loss of generality, from now on, the viscosity to be equal unity.

Additionally to the inverse problem of detecting the unknown point-wise sources, one has to complete the boundary data, that is to recover the missing traces of the velocity  $u$  and of the normal stress  $\sigma(u, p)n$  over  $\bar{\Gamma}_i$ , the inaccessible part of the boundary. This inverse problem is of Cauchy type, a family of problems known to be severely ill-posed in the sense of Hadamard [19], even regardless of the point-wise force identification, because the existence of solution is not guaranteed for arbitrary Cauchy data and depends on their *compatibility*, and even if a solution exists, it is unstable with respect to small perturbations of the Cauchy data.

For the Cauchy problem, there exists a prolific dedicated literature. An excerpt of popular approaches are the least-square penalty techniques, as used in [14] and in the earlier paper [16], Tikhonov regularization methods [9], quasi reversibility methods [6], alternating iterative methods [22, 23] and control type methods [1, 27]. Recently, an approach based on game theory, using decentralized strategies, was proposed in [17]. The same approach has been investigated in [8] for the solution of coupled conductivity identification and data completion in cardiac electrophysiology, and in [18] to solve the problem of detecting unknown cavities immersed in a stationary viscous fluid using partial boundary measurements.

The point-wise force identification for the Stokes system was, in contrast, paid much less attention. Due to the singularity of the point-wise sources, a convenient formulation would require an *ad hoc* functional framework using weighted spaces, norms and cost functions, see e.g [2]. In [15], the authors proposed to detect the point-force locations by minimizing tracking (a difference to a distributed state known all over  $\Omega$ ) and energy functionals. Their algorithm is based on a relaxation technique and on topological sensitivity analysis, which makes recourse to the classical Sobolev functional framework, eluding the need of weighted spaces. We shall follow the same lines for the source identification algorithmic part of our coupled inverse problem. The authors in [3] introduced an approach based on considering a reciprocity gap functional for *Stokeslets* located outside  $\Omega$ . To the best of our knowledge, there are no papers which address algorithmic aspects in solving the present coupled point-wise source identification and boundary data recovery problems for the steady Stokes flows. The paper [24] addresses the coupled inverse problem of identifying wells and recovering boundary data, but with the help of a number of interior measurements. We can also mention an

1 earlier paper made by El Badia and Ha-Duong [11] for an inverse source problem for elliptic equations. Its  
 2 application aims to identify electrostatic dipoles in the human head where the boundary data are generated  
 3 via electrodes placed on the head's part. The authors give a uniqueness result and an algebraic method for  
 4 computing the number of dipoles and their characteristics.

5  
 6 The paper is organized as follows. In section 2, we introduce the identifiability problem for the Cauchy-  
 7 Stokes case, and we provide an identifiability result. Then, using a relaxed formulation in section 3, we  
 8 formulate a Nash game approach to tackle the coupled problem of detecting the unknown point-forces and  
 9 recovering the missing boundary data. A topological sensitivity analysis method is used in order to determine  
 10 the optimal location of the point-sources. We present what we think is a fairly new algorithm. Optimization  
 11 (sub)tasks are performed by means of descend methods, so *ad hoc* adjoint state methods are provided to  
 12 compute the gradients.

13 Finally, Section 4 illustrates the efficiency and robustness of the proposed overall method, where different  
 14 numerical experiments are presented and discussed. We end paper by a short concluding section.

15  
 16 **Some notation:** Let  $\Omega$  be a bounded domain in  $\mathbb{R}^d$  ( $d=2$  or  $3$ ), with Lipschitz boundary  $\partial\Omega$ . Let  $\Gamma_c$  be  
 17 an open part of  $\partial\Omega$  and we put  $\Gamma_i = \partial\Omega \setminus \Gamma_c$ . For any subset  $\Gamma = \Gamma_c$  or  $\Gamma_i$ , the space of function in  $H^1(\Omega)^d$   
 18 vanishing on  $\Gamma$  is denoted by  $H_\Gamma^1(\Omega)$ . By  $H^{\frac{1}{2}}(\Gamma)^d$ , we denote the space of traces of functions of  $H^1(\Omega)^d$  over  
 19  $\Gamma$ . Furthermore, we will use the special space  $H_{00}^{\frac{1}{2}}(\Gamma)^d$ , which consists of functions from  $H^{\frac{1}{2}}(\Gamma)^d$  vanishing  
 20 on  $\partial\Omega \setminus \Gamma$ . This is a subspace of  $H^{\frac{1}{2}}(\Gamma)^d$  and its dual space is then denoted by  $(H_{00}^{\frac{1}{2}}(\Gamma)^d)'$ .

## 21 2. An identifiability result for the inverse point-forces Cauchy-Stokes problem

22 The source identifiability problem amounts to ask whether a unique pair of over specified boundary data,  
 23 for instance the Cauchy data  $(G, \Phi)$ , could reconstruct a unique source, and if not, how much of such pairs  
 24 is necessary to a unique reconstruction.

25 Our identifiability result is given by the following theorem:

26 **Theorem 1.** *Let be  $\Omega \subset \mathbb{R}^d$  an open bounded Lipschitz domain and  $\Gamma_c$  a non-empty open subset of the*  
 27 *boundary  $\partial\Omega$ . Consider two point-wise source terms  $F_1$  and  $F_2$  of the form (1), whose magnitudes and*  
 28 *locations satisfy the requirements stated in (2).*

For  $i = 1, 2$ , let be  $(u_i, p_i)$  the solution of the following :

$$29 \left\{ \begin{array}{ll} -\operatorname{div}(\sigma(u_i, p_i)) & = F_i \quad \text{in } \Omega, \\ \operatorname{div} u_i & = 0 \quad \text{in } \Omega, \\ u_i & = G \quad \text{on } \Gamma_c, \\ \sigma(u_i, p_i)n & = \Phi \quad \text{on } \Gamma_c. \end{array} \right. \quad (3)$$

where the Cauchy data  $(G, \Phi) \in H^{\frac{1}{2}}(\Gamma_c)^d \times (H_{00}^{\frac{1}{2}}(\Gamma_c)^d)'$  are assumed to be compatible for the two Cauchy-  
 Stokes problems. Then  $F_1 = F_2$ , that is,

$$30 m_1 = m_2 = m, \quad \{(\lambda_{k,1}, P_{k,1}), 1 \leq k \leq m\} = \{(\lambda_{k',2}, P_{k',2}), 1 \leq k' \leq m\}.$$

31 *Proof:* An identifiability result is proved for the Dirac-Stokes problem in [3] using the reciprocity gap.  
 32 In our general framework, proofs of identifiability usually follow the same classical steps by properly using  
 33 the unique continuation property, notably for second order elliptic PDES. We follow the same lines, with  
 slight adaption to our Cauchy-Stokes problem.

Let  $(u_i, p_i)$ ,  $i=1,2$  be solutions to the system (3), and we define  $(v, q) = (u_1 - u_2, p_1 - p_2)$  and  $F = F_1 - F_2$ ,  
 where

$$F = \sum_{k=1}^{m_1} \lambda_{k,1} \delta_{P_{k,1}} - \sum_{k'=1}^{m_2} \lambda_{k',2} \delta_{P_{k',2}}, \quad \forall k, k' = 1, \dots, m_i \text{ and } i = 1, 2.$$

It is straightforward to see that  $(v, q)$  is a solution of

$$(\mathcal{P}) \begin{cases} -\operatorname{div}(\sigma(v, q)) = F & \text{in } \Omega, \\ \operatorname{div} v = 0 & \text{in } \Omega, \\ v = 0 & \text{on } \Gamma_c, \\ \sigma(v, q)n = 0 & \text{on } \Gamma_c. \end{cases}$$

Consider  $(\mathcal{B}_{k,i})_{k=1,\dots,m_i}$  for  $i = 1, 2$ , a family of open balls such that

$$0 < \epsilon \ll 1, \mathcal{B}_{k,i} = B(P_{k,i}, \epsilon) \subset \Omega, \text{ and } \mathcal{B}_{k,i} \cap \mathcal{B}_{k',i} = \emptyset, \text{ if } k \neq k'. \quad (4)$$

1 Thus  $F$  vanishes as restricted to  $\Omega_H = \Omega \setminus ((\cup_{k=1}^{m_1} \mathcal{B}_{k,1}) \cup (\cup_{k'=1}^{m_2} \mathcal{B}_{k',2}))$ .

2 From the unique continuation theorem for the steady Stokes equation established in [13], we obtain  $v = 0$   
3 and  $q = 0$  in  $\Omega_H$ . Let us suppose that  $m_1 > m_2$ , and as the positions  $P_k$  are well separated and satisfy (2),  
4 then there exists a source  $P_{m_0,1} \neq P_{k',2}$ ,  $k' = 1, \dots, m_2$ , and we define  $\Omega_0 = \Omega \setminus ((\cup_{k \neq m_0} \mathcal{B}_{k,1}) \cup (\cup_{k'=1}^{m_2} \mathcal{B}_{k',2}))$   
5 with  $k = 1, \dots, m_1$ .

6 We denote  $\mathcal{O} = \mathcal{B}_{m_0,1} \subset \Omega$ . Thus, the solution  $(v, q)$  of the problem  $(\mathcal{P})$ , which is null in  $\Omega_0 \setminus \mathcal{O}$ , satisfies  
7 the following system in  $\mathcal{O}$ ;

$$\begin{cases} -\operatorname{div}(\sigma(v, q)) = \lambda_{m_0,1} \delta_{P_{m_0,1}} & \text{in } \mathcal{O}, \\ \operatorname{div} v = 0 & \text{in } \mathcal{O}, \\ v = 0 & \text{on } \partial \mathcal{O}. \end{cases} \quad (5)$$

Let us consider now the solution  $(v_s, q_s)$  that satisfies:

$$\begin{cases} -\operatorname{div}(\sigma(v_s, q_s)) = \lambda_{m_0,1} \delta_{P_{m_0,1}} & \text{in } \mathbb{R}^d, \\ \operatorname{div} v_s = 0 & \text{in } \mathbb{R}^d, \end{cases}$$

and  $(v_r, q_r)$  which solves

$$\begin{cases} -\operatorname{div}(\sigma(v_r, q_r)) = 0 & \text{in } \mathcal{O}, \\ \operatorname{div} v_r = 0 & \text{in } \mathcal{O}, \\ v_r = -v_s & \text{on } \partial \mathcal{O}. \end{cases}$$

Thus, the solution  $(v_s, q_s)$  is given by

$$(v_s, q_s) = (U * (\lambda_{m_0,1} \delta_{P_{m_0,1}}), P * (\lambda_{m_0,1} \delta_{P_{m_0,1}})) = (U(\cdot - P_{m_0,1}) \cdot \lambda_{m_0,1}, P(\cdot - P_{m_0,1}) \cdot \lambda_{m_0,1}),$$

where the pair  $(U, P)$  is the fundamental solution of the Stokes equation. It is given (see e.g. [3]), for  $d = 2$ ,  
by

$$\begin{cases} U_{ij}(x) = \frac{1}{4\pi\nu} \left( \delta_{ij} \log\left(\frac{1}{|x|}\right) + \frac{x_i x_j}{|x|^2} \right), & i, j = 1, 2 \\ P_i(x) = \frac{1}{2\pi} \frac{x_i}{|x|^2}, & i = 1, 2 \end{cases}$$

and, for  $d = 3$ ,

$$\begin{cases} U_{ij}(x) = \frac{1}{8\pi\nu} \left( \delta_{ij} \left(\frac{1}{|x|}\right) + \frac{x_i x_j}{|x|^3} \right), & i, j = 1, 2, 3 \\ P_i(x) = \frac{1}{4\pi} \frac{x_i}{|x|^3}, & i = 1, 2, 3. \end{cases}$$

8 Then, we can deduce that the solution  $(v, q)$  of the problem  $(\mathcal{P})$ , and which satisfies (5), can be written  
9  $(v, q) = (v_r + v_s, q_r + q_s)$  in  $\mathcal{O}$ . Besides, we have  $(v_s, q_s)$  is an analytic solution in  $\mathcal{O} \setminus P_{m_0,1}$ , implies that  $v_s$   
10 is analytic on the boundary of  $\mathcal{O}$ , then  $v_r$  is an analytic function in  $\mathcal{O} \setminus P_{m_0,1}$ . Therefore, the fluid velocity  
11  $v$ , which is null in  $\Omega_0 \setminus \mathcal{O}$ , is an analytic function in  $\mathcal{O} \setminus P_{m_0,1}$ . This would imply that  $\lambda_{m_0,1} = 0$ , which by  
12 assumption is impossible.

13

1 We proceed analogously, for the case  $m_2 > m_1$ . Thus,  $m = m_1 = m_2$ .

2 Now, let us suppose

$$\{P_{1,1}, \dots, P_{m,1}\} \neq \{P_{1,2}, \dots, P_{m,2}\},$$

and we assume that  $\mathcal{O}$  is a subset of  $\Omega$  such that  $\{\cup_{k=1}^m (P_{k,1} \cup P_{k,2})\} \in \mathcal{O}$ . In the same way, we deduce that the solution  $v$  is an analytic function in  $\mathcal{O} \setminus \{\cup_{k=1}^m (P_{k,1} \cup P_{k,2})\}$ , which is null in  $\Omega \setminus \mathcal{O}$ , and by application of the unique continuation property we conclude that  $v$  equal to zero in  $\mathcal{O}$ , that is,

$$\sum_{k=1}^m (\lambda_{k,1} \delta_{P_{k,1}} - \lambda_{k,2} \delta_{P_{k,2}}) = 0 \text{ in } \mathcal{O},$$

such that  $\lambda_{k,i} \neq 0$  for  $k = 1, \dots, m$  and  $i=1,2$ . Therefore, there exists a unique permutation  $\pi$  of the entries such that,

$$P_{k,1} = P_{\pi(k),2}, \forall k = \{1, \dots, m\}.$$

3 Finally, we conclude that  $F = \sum_{k=1}^m (\lambda_{k,1} - \lambda_{\pi(k),2}) \delta_{P_{k,2}}$ . Using the same arguments, we obtain  $\lambda_{k,1} = \lambda_{\pi(k),2}$ ,  
4 with  $i=1,2$  and  $k = 1, \dots, m$ . ■

### 6 3. A game formulation of the coupled data completion and point-forces identification problems

7 With the previous notations, let be  $G \in H^{\frac{1}{2}}(\Gamma_c)^d$  and  $\Phi \in (H_{00}^{\frac{1}{2}}(\Gamma_c)^d)'$  given Cauchy data. We recall that  
8 the inverse source-term problem amounts to find a collection of point-wise sources  $F^* \in H^s(\Omega)^d$  for  $s < -1$   
9 such that the fluid velocity  $u$  and the pressure  $p$  are solution to the following Cauchy-Stokes problem:

$$(\mathcal{CS}) \begin{cases} -\operatorname{div}(\sigma(u, p)) = F^* & \text{in } \Omega, \\ \operatorname{div} u = 0 & \text{in } \Omega, \\ u = G & \text{on } \Gamma_c, \\ \sigma(u, p)n = \Phi & \text{on } \Gamma_c. \end{cases}$$

10 For any given  $\eta \in (H_{00}^{\frac{1}{2}}(\Gamma_i)^d)'$ ,  $\tau \in H^{\frac{1}{2}}(\Gamma_i)^d$  and  $F \in H^s(\Omega)^d$  for  $s < -1$ , we define the states  $(u_1, p_1) =$   
11  $(u_1(\eta, F), p_1(\eta, F)) \in L^2(\Omega)^d \times L^2(\Omega)$  and  $(u_2, p_2) = (u_2(\tau, F), p_2(\tau, F)) \in L^2(\Omega)^d \times L^2(\Omega)$  as the unique  
12 solution of the following Stokes mixed boundary value problem  $(\mathcal{P}_1)$  and  $(\mathcal{P}_2)$ ,

$$(\mathcal{P}_1) \begin{cases} -\operatorname{div}(\sigma(u_1, p_1)) = F & \text{in } \Omega, \\ \operatorname{div} u_1 = 0 & \text{in } \Omega, \\ u_1 = G & \text{on } \Gamma_c, \\ \sigma(u_1, p_1)n = \eta & \text{on } \Gamma_i, \end{cases} \quad (\mathcal{P}_2) \begin{cases} -\operatorname{div}(\sigma(u_2, p_2)) = F & \text{in } \Omega, \\ \operatorname{div} u_2 = 0 & \text{in } \Omega, \\ u_2 = \tau & \text{on } \Gamma_i, \\ \sigma(u_2, p_2)n = \Phi & \text{on } \Gamma_c. \end{cases}$$

13 The proof of the existence and uniqueness of the solutions to  $(\mathcal{P}_1)$  and  $(\mathcal{P}_2)$ , can be easily adapted from  
14 the proof given in [15] for the Dirichlet type boundary condition. Since the source  $F$  given by (1) belongs  
15 to Hilbert space  $H^s(\Omega)^d$  with  $s < -1$ , a classical formulation of the problems  $(\mathcal{P}_1)$  and  $(\mathcal{P}_2)$ , well adapted  
16 to standard finite elements analysis is not possible. Nevertheless, to overcome this difficulty, we recourse to  
17 a relaxation technique, which consists in approximating the point-force support  $P_k$  by a small region, we  
18 could also use a subtraction method [3].

1 3.1. Relaxation step

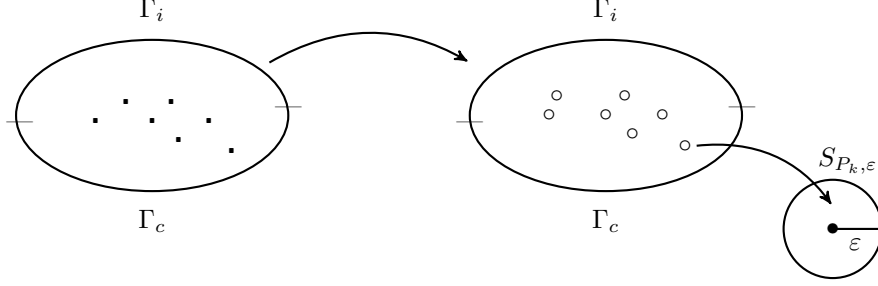


Figure 1: Relaxation step

We consider the classical approximation of a Dirac function at a points  $P = \{P_1, \dots, P_m\}$  by the characteristic function of a small ball centred at  $P$  divided by its volume. Thus, instead of the source term  $F$  given by (1), we consider the following:

$$F_\epsilon = \sum_{k=1}^m \frac{\lambda_k}{|\mathcal{S}_{P_k, \epsilon}|} \chi_{\mathcal{S}_{P_k, \epsilon}}$$

where  $\chi_{\mathcal{S}_{P_k, \epsilon}}$  denotes the characteristic function of the ball  $\mathcal{S}_{P_k, \epsilon} = P_k + \epsilon\omega_k$ , with  $\epsilon > 0$  is small enough and  $\omega_k$  is bounded and smooth domain containing the origin. As the positions  $P_k$  are well separated and satisfy (2), we can suppose then that the region  $\mathcal{S}_{P_k, \epsilon}$  also do not intersect,

$$\mathcal{S}_{P_k, \epsilon} \cap \mathcal{S}_{P_{k'}, \epsilon} = 0 \text{ if } k \neq k'. \quad (6)$$

The set of admissible source term  $\mathcal{D}_{\text{ad}}$  is defined by:

$$\mathcal{D}_{\text{ad}} = \left\{ f \in L^2(\Omega); f = \sum_{k=1}^p \beta_k \chi_{\mathcal{S}_{z_k, \epsilon}}, \text{ such that } \mathcal{S}_{z_k, \epsilon} \subset\subset \Omega \right\}.$$

Problems  $(\mathcal{P}_1)$  and  $(\mathcal{P}_2)$  are then rephrased in terms of this more regular source term. Let  $(u_{1, \epsilon}, p_{1, \epsilon}) \in H^1(\Omega)^d \times L^2(\Omega)$  and  $(u_{2, \epsilon}, p_{2, \epsilon}) \in H^1(\Omega)^d \times L^2(\Omega)$  be the unique solutions of the respective relaxed BVPs  $(\mathcal{P}_{1, \epsilon})$  and  $(\mathcal{P}_{2, \epsilon})$ ,

$$\begin{aligned} (\mathcal{P}_{1, \epsilon}) & \begin{cases} -\text{div}(\sigma(u_{1, \epsilon}, p_{1, \epsilon})) = F_\epsilon & \text{in } \Omega, \\ \text{div} u_{1, \epsilon} = 0 & \text{in } \Omega, \\ u_{1, \epsilon} = G & \text{on } \Gamma_c, \\ \sigma(u_{1, \epsilon}, p_{1, \epsilon})n = \eta & \text{on } \Gamma_i, \end{cases} \\ (\mathcal{P}_{2, \epsilon}) & \begin{cases} -\text{div}(\sigma(u_{2, \epsilon}, p_{2, \epsilon})) = F_\epsilon & \text{in } \Omega, \\ \text{div} u_{2, \epsilon} = 0 & \text{in } \Omega, \\ \sigma(u_{2, \epsilon}, p_{2, \epsilon})n = \Phi & \text{on } \Gamma_c, \\ u_{2, \epsilon} = \tau & \text{on } \Gamma_i, \end{cases} \end{aligned}$$

where

$$F_\epsilon = \sum_{k=1}^m \frac{\lambda_k}{|\mathcal{S}_{P_k, \epsilon}|} \chi_{\mathcal{S}_{P_k, \epsilon}} \in \mathcal{D}_{\text{ad}} \quad (7)$$

2 is more regular source term, with  $\chi_{\mathcal{S}_{P_k, \epsilon}}$  is the characteristic function of the unknown region  $\mathcal{S}_{P_k, \epsilon}$ .

1 **Remark 1.** The existence and uniqueness of the solutions  $(\mathcal{P}_{1,\epsilon})$  and  $(\mathcal{P}_{2,\epsilon})$ , can be derived from the general  
 2 theory on existence of solutions to the incompressible steady state Stokes equations, which can be found  
 3 e.g. in [10, 28]; See also [5] which is suitable to the Stokes framework of the present paper. Moreover,  
 4 the solutions  $(u_{1,\epsilon}, p_{1,\epsilon})$  and  $(u_{2,\epsilon}, p_{2,\epsilon})$  converge to the respective solutions  $(u_1, p_1)$  and  $(u_2, p_2)$  with the  
 5 parameter  $\epsilon$ , the proof of this result can be handled by applying the same technique as in [15].

6  
 7 Let  $\mathcal{I}_{\text{ad}} = \{(m; \lambda, P) \in \mathbb{N}^* \times \mathbb{R}^{dm} \times \Omega^m\}$ . Let  $\phi = (m; (\lambda_k, P_k)_{1 \leq k \leq m}) \in \mathcal{I}_{\text{ad}}$  be a source configuration  
 8 corresponding to a source  $F$  of the form (1). Let us introduce the following three cost functionals:

$$\mathcal{J}_1(\eta, \tau; \phi) = \frac{1}{2} \|\sigma(u_{1,\epsilon}, p_{1,\epsilon})n - \Phi\|_{(H_{00}^{\frac{1}{2}}(\Gamma_i)^d)'}^2 + \frac{\alpha}{2} \|u_{1,\epsilon} - u_{2,\epsilon}\|_{H^{\frac{1}{2}}(\Gamma_i)^d}^2, \quad (8)$$

$$\mathcal{J}_2(\eta, \tau; \phi) = \frac{1}{2} \|u_{2,\epsilon} - G\|_{H^{\frac{1}{2}}(\Gamma_i)^d}^2 + \frac{\alpha}{2} \|u_{1,\epsilon} - u_{2,\epsilon}\|_{H^{\frac{1}{2}}(\Gamma_i)^d}^2, \quad (9)$$

$$\mathcal{J}_3(\eta, \tau; \phi) = \|\sigma(u_{1,\epsilon}, p_{1,\epsilon}) - \sigma(u_{2,\epsilon}, p_{2,\epsilon})\|_{L^2(\Omega)^d}^2, \quad (10)$$

9 where  $\alpha$  is given positive parameter (e.g.  $\alpha = 1$ ). Player (1) controls the strategy variable  $\eta \in (H_{00}^{\frac{1}{2}}(\Gamma_i)^d)'$   
 10 and aims at minimizing the cost  $\mathcal{J}_1$  and Player (2) controls the strategy variable  $\tau \in H^{\frac{1}{2}}(\Gamma_i)^d$  and aims at  
 11 minimizing the cost  $\mathcal{J}_2$ : they are given Dirichlet (resp. Neumann) data and try to minimize the gap with  
 12 the Neumann (resp. Dirichlet) remaining condition. The player (3) controls the strategy variable  $\phi \in \mathcal{I}_{\text{ad}}$   
 13 and aims at minimizing the Kohn-Vogelius type functional  $\mathcal{J}_3$ .

14 **Definition 1.** A triplet  $(\eta_N, \tau_N, \phi_N) \in (H_{00}^{\frac{1}{2}}(\Gamma_i)^d)' \times H^{\frac{1}{2}}(\Gamma_i)^d \times \mathcal{I}_{\text{ad}}$  is a Nash equilibrium for the three players  
 15 game if the following holds:

$$\begin{cases} \mathcal{J}_1(\eta_N, \tau_N; \phi_N) \leq \mathcal{J}_1(\eta, \tau_N, \phi_N), & \forall \eta \in (H_{00}^{\frac{1}{2}}(\Gamma_i)^d)', \\ \mathcal{J}_2(\eta_N, \tau_N; \phi_N) \leq \mathcal{J}_2(\eta_N, \tau, \phi_N), & \forall \tau \in H^{\frac{1}{2}}(\Gamma_i)^d, \\ \mathcal{J}_3(\eta_N, \tau_N; \phi_N) \leq \mathcal{J}_3(\eta_N, \tau_N, \phi), & \forall \phi \in \mathcal{I}_{\text{ad}}. \end{cases} \quad (11)$$

16  
 The player 3 in charge of the inverse source-term problem has as a strategy  $\phi = (m; (\lambda_k, P_k)_{1 \leq k \leq m})$ ,  
 which is a solution of the following optimization problem,

$$\min_{\phi \in \mathcal{I}_{\text{ad}}} \mathcal{J}_3(\eta, \tau; \phi), \quad \text{when } (\eta, \tau) \in (H_{00}^{\frac{1}{2}}(\Gamma_i)^d)' \times H^{\frac{1}{2}}(\Gamma_i)^d.$$

17 In the following, the player (3) will play in two steps in order to determine the elements defining the  
 18 source  $F$  introduced in (1); a first step enables to localize the source position  $P = \{P_1, \dots, P_m\}$ , or in other  
 19 words after this relaxation step, the support of  $\mathcal{S} = \cup_{k=1}^m \mathcal{S}_{k,\epsilon}$ . Then, a second step uses the determined  
 20 source position and compute the approximate value of the source intensity  $\Lambda = \{\lambda_1, \dots, \lambda_m\}$ .

### 21 3.2. Localization of the source position.

Here, the player (3) focuses on identifying the optimal location of the source-term with respect to the  
 assumption (6). Therefore, the minimization problem of  $\mathcal{J}_3$  w.r.t.  $P$  can be formulated as a topological op-  
 timization one. Thus, the unknown region  $\mathcal{S}$  can be characterized as the solution to the following topological  
 optimization problem, for fixed  $(\eta, \tau, \Lambda) \in (H_{00}^{\frac{1}{2}}(\Gamma_i)^d)' \times H^{\frac{1}{2}}(\Gamma_i)^d \times \mathbb{R}^{dm}$ ,

$$\left\{ \begin{array}{l} \text{Find } \mathcal{S}^* = \cup_{k=1}^m \mathcal{S}_{P_k, \epsilon} \subset \Omega, \text{ such that} \\ \mathcal{S}^* = \arg \min_{\mathcal{S} \subset \Omega} \left\{ \mathcal{J}(\mathcal{S}) := \int_{\Omega} |\sigma(u_{1,\epsilon}, p_{1,\epsilon}) - \sigma(u_{2,\epsilon}, p_{2,\epsilon})|^2 dx \right\}, \end{array} \right.$$

22 where  $(u_{1,\epsilon}, p_{1,\epsilon})$  and  $(u_{2,\epsilon}, p_{2,\epsilon})$  are the solutions to respectively  $(\mathcal{P}_{1,\epsilon})$  and  $(\mathcal{P}_{2,\epsilon})$ . In order to solve this  
 23 problem, we shall use a topological sensitivity analysis method. The concept of the topological derivative



1 was proposed by Schumacher et al. [12] in the case of compliance minimization. Next, Sokolowski et al.  
2 [26] extended it to more general shape functionals. It consists of studying the variation of the cost function  
3 with respect to small perturbations of the domain's topology. It has been widely applied in literature for  
4 arbitrarily shaped perturbations and a general class of cost functionals related to PDEs. In our case, we  
5 want to apply the topological gradient computation to adding a source term of a given form to the Stokes  
6 equations. A topological gradient computation for a source term perturbation can be found in [15, 25].

### 7 3.2.1. Topological sensitivity method

This approach's main step consists of studying the variation of a given functional with respect to a small  
topological perturbation of the source term. For a given source term  $f$ , let  $\delta f_{P,\epsilon}$  be a finite topological  
perturbation of  $f$  on the form

$$\delta f_{P,\epsilon} = \begin{cases} \lambda & \text{in } \omega_{P,\epsilon} = \cup_{k=1}^m \omega_{P_k,\epsilon} \\ 0 & \text{in } \Omega \setminus \overline{\cup_{k=1}^m \omega_{P_k,\epsilon}} \end{cases}$$

8 where  $P = (P_1, \dots, P_m) \in \Omega^m$ , and  $\omega_{P_k,\epsilon}$ ,  $1 \leq k \leq m$  are small geometrical perturbation separated and  
9 have the geometry form  $\omega_{P_k,\epsilon} = P_k + \epsilon B$ , where  $\epsilon > 0$  is small enough and  $B$  is a fixed bounded domain  
10 containing the origin. The points  $P_k \in \Omega$ ,  $1 \leq k \leq m$ , determine the location of the geometric  $\omega_{P_k,\epsilon}$ .

11 Then, the asymptotic expansion of the given cost function  $\mathcal{J}$  with respect to  $\epsilon$  takes the form,

$$\begin{aligned} \mathcal{J}(f + \delta f_{P,\epsilon}) - \mathcal{J}(f) &= \rho(\epsilon) \sum_{k=1}^m \mathcal{G}(P_k) + o(\rho(\epsilon)), \quad \forall P_k \in \Omega, \\ \lim_{\epsilon \rightarrow 0} \rho(\epsilon) &= 0, \quad \rho(\epsilon) > 0, \end{aligned} \quad (12)$$

where the function  $\mathcal{G}$  is the so-called topological gradient. Therefore, the source location would be identified  
in the region where the topological gradient is the most negative, that means that, the function  $\mathcal{J}$  will be  
decreased if we add source terms at points  $P_k$ ,  $1 \leq k \leq m$ .

Let us consider, for now, the case of a single support  $\mathcal{S}_{x_0,\epsilon} := \omega_{x_0,\epsilon}$  such that the perturbation  $\delta f_\epsilon := \delta f_{x_0,\epsilon}$   
is given by

$$\delta f_\epsilon = \begin{cases} \lambda & \text{in } \mathcal{S}_{x_0,\epsilon}, \\ 0 & \text{in } \Omega \setminus \overline{\mathcal{S}_{x_0,\epsilon}}. \end{cases}$$

Then, we define the source function  $\mathcal{J}$  to be minimized,

$$\mathcal{J}(f + \delta f_\epsilon) := \mathcal{J}((u_1^\epsilon, p_1^\epsilon); (u_2^\epsilon, p_2^\epsilon)),$$

where

$$\mathcal{J}((u_1^\epsilon, p_1^\epsilon); (u_2^\epsilon, p_2^\epsilon)) = \int_{\Omega} |\sigma(u_1^\epsilon, p_1^\epsilon) - \sigma(u_2^\epsilon, p_2^\epsilon)|^2 dx,$$

and  $(u_1^\epsilon, p_1^\epsilon)$  and  $(u_2^\epsilon, p_2^\epsilon)$  are respective solutions of the following BVP,

$$(P_1^\epsilon) \begin{cases} -\operatorname{div}(\sigma(u_1^\epsilon, p_1^\epsilon)) &= f + \delta f_\epsilon & \text{in } \Omega, \\ \operatorname{div} u_1^\epsilon &= 0 & \text{in } \Omega, \\ u_1^\epsilon &= G & \text{on } \Gamma_c, \\ \sigma(u_1^\epsilon, p_1^\epsilon)n &= \eta & \text{on } \Gamma_i, \end{cases} \quad (P_2^\epsilon) \begin{cases} -\operatorname{div}(\sigma(u_2^\epsilon, p_2^\epsilon)) &= f + \delta f_\epsilon & \text{in } \Omega, \\ \operatorname{div} u_2^\epsilon &= 0 & \text{in } \Omega, \\ \sigma(u_2^\epsilon, p_2^\epsilon)n &= \Phi & \text{on } \Gamma_c, \\ u_2^\epsilon &= \tau & \text{on } \Gamma_i, \end{cases}$$

Then, the weak solutions to problem  $(P_1^\epsilon)$  and  $(P_2^\epsilon)$  are defined by:

$$\begin{cases} \text{Find } (u_1^\epsilon, p_1^\epsilon) \in H^1(\Omega)^d \times L^2(\Omega) \text{ such that,} \\ \mathcal{A}(u_1^\epsilon, \varphi_1) + \mathcal{B}(p_1^\epsilon, \varphi_1) &= l_{1,\epsilon}(\varphi_1), \quad \forall \varphi_1 \in H_{\Gamma_c}^1(\Omega), \\ \mathcal{B}(\xi_1, u_1^\epsilon) &= 0, \quad \forall \xi_1 \in L_0^2(\Omega), \end{cases} \quad (13)$$

$$\left\{ \begin{array}{l} \text{Find } (u_2^\epsilon, p_2^\epsilon) \in H^1(\Omega)^d \times L^2(\Omega) \text{ such that,} \\ \mathcal{A}(u_2^\epsilon, \varphi_2) + \mathcal{B}(p_2^\epsilon, \varphi_2) = l_{2,\epsilon}(\varphi_2), \quad \forall \varphi_2 \in H_{\Gamma}^1(\Omega), \\ \mathcal{B}(\xi_2, u_2^\epsilon) = 0, \quad \forall \xi_2 \in L_0^2(\Omega), \end{array} \right. \quad (14)$$

where

$$\mathcal{A}(u_i^\epsilon, \varphi_i) = \int_{\Omega} D(u_i^\epsilon) : \nabla \varphi_i \, dx, \quad \mathcal{B}(p_i^\epsilon, \varphi_i) = - \int_{\Omega} p_i^\epsilon \operatorname{div} \varphi_i \, dx$$

and

$$l_{1,\epsilon}(\varphi_1) = \int_{\Omega} (f + \delta f_\epsilon) \varphi_1 \, dx + \int_{\Gamma_i} \eta \varphi_1 \, ds, \quad l_{2,\epsilon}(\varphi_2) = \int_{\Omega} (f + \delta f_\epsilon) \varphi_2 \, dx + \int_{\Gamma_c} \Phi \varphi_2 \, ds.$$

We now consider the case where  $f = 0$ , then, the linear forms  $l_{1,0}$  and  $l_{2,0}$  can be defined as follows

$$l_{1,0}(\varphi_1) = \int_{\Gamma_i} \eta \varphi_1 \, ds, \quad l_{2,0}(\varphi_2) = \int_{\Gamma_c} \Phi \varphi_2 \, ds.$$

1  
2 Next, we introduce the following proposition which describes an adjoint method, for the computation of  
3 this first variation of our cost function  $\mathcal{J}$  with respect to  $\epsilon$ .

4 **Proposition 1.** Consider  $(u_1^\epsilon, p_1^\epsilon)$  and  $(u_2^\epsilon, p_2^\epsilon)$  solutions of the Problems (13) and (14), respectively. Sup-  
5 pose that the following assumptions hold:

6 (i)  $\mathcal{J}$  is Fréchet-differentiable with respect to  $(u_i, p_i)$ , for  $i = 1, 2$ .

7 (ii) There exist two real numbers  $\delta l_1$  and  $\delta l_2$  such that

$$(l_{1,\epsilon} - l_{1,0})(v_1) = \rho(\epsilon) \delta l_1 + o(\rho(\epsilon)),$$

$$(l_{2,\epsilon} - l_{2,0})(v_2) = \rho(\epsilon) \delta l_2 + o(\rho(\epsilon)),$$

8 where  $(v_1, q_1)$  and  $(v_2, q_2)$  are solutions of the following weak formulations adjoint problems,

$$(\mathcal{AP}_1) \left\| \begin{array}{l} \mathcal{A}(h_1, v_1) + \mathcal{B}(k_1, v_1) - \mathcal{B}(q_1, h_1) = - \frac{\partial \mathcal{J}}{\partial u_1}((u_1^0, p_1^0); (u_2^0, p_2^0)).h_1 - \frac{\partial \mathcal{J}}{\partial p_1}((u_1^0, p_1^0); (u_2^0, p_2^0)).k_1 \end{array} \right.$$

$$(\mathcal{AP}_2) \left\| \begin{array}{l} \mathcal{A}(h_2, v_2) + \mathcal{B}(k_2, v_2) - \mathcal{B}(q_2, h_2) = - \frac{\partial \mathcal{J}}{\partial u_2}((u_1^0, p_1^0); (u_2^0, p_2^0)).h_2 - \frac{\partial \mathcal{J}}{\partial p_2}((u_1^0, p_1^0); (u_2^0, p_2^0)).k_2 \end{array} \right.$$

9 for all  $(h_1, k_1) \in H_{\Gamma_c}^1(\Omega) \times L^2(\Omega)$  and  $(h_2, k_2) \in H_{\Gamma_i}^1(\Omega) \times L^2(\Omega)$ .

Then the first variation of the cost function  $\mathcal{J}$  with respect to  $\epsilon$  is given by,

$$\mathcal{J}(\delta f_\epsilon) = \mathcal{J}(0) + \rho(\epsilon)(\delta l_1 + \delta l_2) + o(\rho(\epsilon)),$$

where  $\rho(\epsilon) = |\mathcal{S}_{x_0, \epsilon}|$ . The topological gradient  $\mathcal{G}$  at point  $x_0$  is given by:

$$\mathcal{G}(x_0) = -\lambda.(v_1 + v_2)(x_0), \quad (15)$$

10 where  $\lambda$  is a constant vector and  $(v_i, q_i)$  is the solution of the adjoint problem  $(\mathcal{AP}_i)$ , with  $i=1,2$ .

11  
12 *Proof.* Let us define the Lagrangian  $\mathcal{L}$  by,

$$\begin{aligned} \mathcal{L}_\epsilon(v_1, q_1, v_2, q_2, u_1, p_1, u_2, p_2) &= \mathcal{J}((u_1, p_1); (u_2, p_2)) + \mathcal{A}(u_1, v_1) + \mathcal{B}(p_1, v_1) \\ &\quad - \mathcal{B}(q_1, u_1) - l_{1,\epsilon}(v_1) + \mathcal{A}(u_2, v_2) + \mathcal{B}(p_2, v_2) - \mathcal{B}(q_2, u_2) - l_{2,\epsilon}(v_2), \end{aligned}$$

with  $(u_1, u_2, v_1, v_2) \in H^1(\Omega)^d \times H^1(\Omega)^d \times H_{\Gamma_c}^1(\Omega) \times H_{\Gamma_f}^1(\Omega)$  and  $(p_1, p_2, q_1, q_2) \in L^2(\Omega)^4$ . Using (13) and (14), we obtain

$$\mathcal{J}(\delta f_\epsilon) = \mathcal{L}_\epsilon(v_1, q_1, v_2, q_2, u_1^\epsilon, p_1^\epsilon, u_2^\epsilon, p_2^\epsilon).$$

So the first variation of the cost function with respect to  $\epsilon$  is given by:

$$\begin{aligned} \mathcal{J}(\delta f_\epsilon) - \mathcal{J}(0) &= \mathcal{L}_\epsilon(v_1, q_1, v_2, q_2, u_1^\epsilon, p_1^\epsilon, u_2^\epsilon, p_2^\epsilon) - \mathcal{L}_0(v_1, q_1, v_2, q_2, u_1^0, p_1^0, u_2^0, p_2^0) \\ &= \mathcal{A}(u_1^\epsilon, v_1) + \mathcal{B}(p_1^\epsilon, v_1) - \mathcal{B}(q_1, u_1^\epsilon) - \mathcal{A}(u_1^0, v_1) - \mathcal{B}(p_1^0, v_1) + \mathcal{B}(q_1, u_1^0) \\ &\quad + \mathcal{A}(u_2^\epsilon, v_2) + \mathcal{B}(p_2^\epsilon, v_2) - \mathcal{B}(q_2, u_2^\epsilon) - \mathcal{A}(u_2^0, v_2) - \mathcal{B}(p_2^0, v_2) + \mathcal{B}(q_2, u_2^0) \\ &\quad - (l_1^\epsilon - l_1^0)(v_1) - (l_2^\epsilon - l_2^0)(v_2) + \mathcal{J}((u_1^\epsilon, p_1^\epsilon); (u_2^\epsilon, p_2^\epsilon)) - \mathcal{J}((u_1^0, p_1^0); (u_2^0, p_2^0)) \end{aligned}$$

1 Then, from the definition of  $\mathcal{A}$  and  $\mathcal{B}$ , we have

$$\begin{aligned} &\mathcal{A}(u_1^\epsilon, v_1) + \mathcal{B}(p_1^\epsilon, v_1) - \mathcal{B}(q_1, u_1^\epsilon) - \mathcal{A}(u_1^0, v_1) - \mathcal{B}(p_1^0, v_1) \\ &\quad + \mathcal{B}(q_1, u_1^0) = \int_{\Omega} D(u_1^\epsilon - u_1^0) : \nabla v_1 \, dx + \int_{\Omega} (p_1^\epsilon - p_1^0) \operatorname{div} v_1 \, dx - \int_{\Omega} q_1 \operatorname{div}(u_1^\epsilon - u_1^0) \, dx, \\ &\mathcal{A}(u_2^\epsilon, v_2) + \mathcal{B}(p_2^\epsilon, v_2) - \mathcal{B}(q_2, u_2^\epsilon) - \mathcal{A}(u_2^0, v_2) - \mathcal{B}(p_2^0, v_2) \\ &\quad + \mathcal{B}(q_2, u_2^0) = \int_{\Omega} D(u_2^\epsilon - u_2^0) : \nabla v_2 \, dx + \int_{\Omega} (p_2^\epsilon - p_2^0) \operatorname{div} v_2 \, dx - \int_{\Omega} q_2 \operatorname{div}(u_2^\epsilon - u_2^0) \, dx. \end{aligned}$$

2 Choosing  $(v_1, q_1)$  and  $(v_2, q_2)$  as the solutions of the adjoints problems  $(\mathcal{AP}_1)$  and  $(\mathcal{AP}_2)$ ,

$$\begin{aligned} &\int_{\Omega} D(u_1^\epsilon - u_1^0) : \nabla v_1 \, dx + \int_{\Omega} (p_1^\epsilon - p_1^0) \operatorname{div} v_1 \, dx - \int_{\Omega} q_1 \operatorname{div}(u_1^\epsilon - u_1^0) \, dx = \\ &\quad - \frac{\partial \mathcal{J}}{\partial u_1}((u_1^0, p_1^0); (u_2^0, p_2^0)) \cdot (u_1^\epsilon - u_1^0) - \frac{\partial \mathcal{J}}{\partial p_1}((u_1^0, p_1^0); (u_2^0, p_2^0)) \cdot (p_1^\epsilon - p_1^0), \\ &\int_{\Omega} D(u_2^\epsilon - u_2^0) : \nabla v_2 \, dx + \int_{\Omega} (p_2^\epsilon - p_2^0) \operatorname{div} v_2 \, dx - \int_{\Omega} q_2 \operatorname{div}(u_2^\epsilon - u_2^0) \, dx = \\ &\quad - \frac{\partial \mathcal{J}}{\partial u_2}((u_1^0, p_1^0); (u_2^0, p_2^0)) \cdot (u_2^\epsilon - u_2^0) - \frac{\partial \mathcal{J}}{\partial p_2}((u_1^0, p_1^0); (u_2^0, p_2^0)) \cdot (p_2^\epsilon - p_2^0). \end{aligned}$$

3 Thus, we have

$$\begin{aligned} \mathcal{J}(\delta f_\epsilon) - \mathcal{J}(0) &= - \frac{\partial \mathcal{J}}{\partial u_1}((u_1^0, p_1^0); (u_2^0, p_2^0)) \cdot (u_1^\epsilon - u_1^0) - \frac{\partial \mathcal{J}}{\partial p_1}((u_1^0, p_1^0); (u_2^0, p_2^0)) \cdot (p_1^\epsilon - p_1^0) \\ &\quad - \frac{\partial \mathcal{J}}{\partial u_2}((u_1^0, p_1^0); (u_2^0, p_2^0)) \cdot (u_2^\epsilon - u_2^0) - \frac{\partial \mathcal{J}}{\partial p_2}((u_1^0, p_1^0); (u_2^0, p_2^0)) \cdot (p_2^\epsilon - p_2^0) \\ &\quad - (l_1^\epsilon - l_1^0)(v_1) - (l_2^\epsilon - l_2^0)(v_2) + \mathcal{J}((u_1^\epsilon, p_1^\epsilon); (u_2^\epsilon, p_2^\epsilon)) - \mathcal{J}((u_1^0, p_1^0); (u_2^0, p_2^0)) \end{aligned}$$

• *Variation of the linear form.* We are interested here in the asymptotic analysis of the variation

$$\begin{aligned} (l_{1,\epsilon} - l_{1,0})(v_1) &= \int_{\Omega} \delta f_\epsilon v_1 \, dx = \int_{\mathcal{S}_{x_0,\epsilon}} \lambda v_1 \, dx, \\ &= |\mathcal{S}_{x_0,\epsilon}| \lambda v_1(x_0) + o(\epsilon). \end{aligned} \tag{16}$$

where  $(v_1, q_1)$  is the solution of the adjoint problem  $(\mathcal{AP}_1)$ . The same, we have

$$(l_{2,\epsilon} - l_{2,0})(v_2) = |\mathcal{S}_{x_0,\epsilon}| \lambda v_2(x_0) + o(\epsilon), \tag{17}$$

4 where  $(v_2, q_2)$  is the solution of the adjoint problem  $(\mathcal{AP}_2)$ .

5

• *Variation of the cost function.* Let us now turn to the asymptotic analysis of the variation of the Kohn-Vogeluis functional given by

$$\mathcal{J}((u_1^\epsilon, p_1^\epsilon); (u_2^\epsilon, p_2^\epsilon)) = \int_{\Omega} |\sigma(u_1^\epsilon, p_1^\epsilon) - \sigma(u_2^\epsilon, p_2^\epsilon)|^2 \, dx.$$

Thus, this functional  $\mathcal{J}$  can be decomposed as

$$\mathcal{J}((u_1^\epsilon, p_1^\epsilon); (u_2^\epsilon, p_2^\epsilon)) = \mathfrak{J}_1(u_1^\epsilon, p_1^\epsilon) + \mathfrak{J}_2(u_2^\epsilon, p_2^\epsilon) - 2\mathfrak{J}_{12}(u_1^\epsilon, p_1^\epsilon; (u_2^\epsilon, p_2^\epsilon)),$$

1 with

$$\mathfrak{J}_1(u_1^\epsilon, p_1^\epsilon) = \int_{\Omega} |\sigma(u_1^\epsilon, p_1^\epsilon)|^2 dx,$$

$$\mathfrak{J}_2(u_2^\epsilon, p_2^\epsilon) = \int_{\Omega} |\sigma(u_2^\epsilon, p_2^\epsilon)|^2 dx,$$

$$\mathfrak{J}_{12}((u_1^\epsilon, p_1^\epsilon); (u_2^\epsilon, p_2^\epsilon)) = \int_{\Omega} \sigma(u_1^\epsilon, p_1^\epsilon) \sigma(u_2^\epsilon, p_2^\epsilon) dx.$$

*Variation of  $\mathfrak{J}_1$ :*

$$\begin{aligned} \mathfrak{J}_1(u_1^\epsilon, p_1^\epsilon) - \mathfrak{J}_1(u_1^0, p_1^0) &= \int_{\Omega} |\sigma(u_1^\epsilon, p_1^\epsilon)|^2 dx - \int_{\Omega} |\sigma(u_1^0, p_1^0)|^2 dx \pm 2 \int_{\Omega} |\sigma(u_1^0, p_1^0)|^2 dx \\ &= \int_{\Omega} |\sigma(u_1^\epsilon, p_1^\epsilon) - \sigma(u_1^0, p_1^0)|^2 dx + 2 \int_{\Omega} \sigma(u_1^\epsilon, p_1^\epsilon) \sigma(u_1^0, p_1^0) dx - 2 \int_{\Omega} |\sigma(u_1^0, p_1^0)|^2 dx. \end{aligned}$$

Posing  $(w_i^\epsilon, \xi_i^\epsilon) = (u_i^\epsilon - u_i^0, p_i^\epsilon - p_i^0)$  for  $i=1,2$ , we obtain

$$\mathfrak{J}_1(u_1^\epsilon, p_1^\epsilon) - \mathfrak{J}_1(u_1^0, p_1^0) = \int_{\Omega} |\sigma(w_1^\epsilon, \xi_1^\epsilon)|^2 dx + 2 \int_{\Omega} \sigma(u_1^0, p_1^0) \sigma(w_1^\epsilon, \xi_1^\epsilon) dx. \quad (18)$$

*Variation of  $\mathfrak{J}_2$ :* In the same way, we find that

$$\mathfrak{J}_2(u_2^\epsilon, p_2^\epsilon) - \mathfrak{J}_2(u_2^0, p_2^0) = \int_{\Omega} |\sigma(w_2^\epsilon, \xi_2^\epsilon)|^2 dx + 2 \int_{\Omega} \sigma(u_2^0, p_2^0) \sigma(w_2^\epsilon, \xi_2^\epsilon) dx. \quad (19)$$

2 *Variation of  $\mathfrak{J}_{12}$ :*

$$\mathfrak{J}_{12}((u_1^\epsilon, p_1^\epsilon); (u_2^\epsilon, p_2^\epsilon)) - \mathfrak{J}_{12}((u_1^0, p_1^0); (u_2^0, p_2^0)) = \int_{\Omega} \sigma(u_1^\epsilon, p_1^\epsilon) \sigma(u_2^\epsilon, p_2^\epsilon) dx - \int_{\Omega} \sigma(u_1^0, p_1^0) \sigma(u_2^0, p_2^0) dx.$$

Then, we have

$$\begin{aligned} \mathfrak{J}_{12}((u_1^\epsilon, p_1^\epsilon); (u_2^\epsilon, p_2^\epsilon)) - \mathfrak{J}_{12}((u_1^0, p_1^0); (u_2^0, p_2^0)) &= \int_{\Omega} \sigma(w_1^\epsilon, \xi_1^\epsilon) \sigma(w_2^\epsilon, \xi_2^\epsilon) dx \\ &\quad + \int_{\Omega} \sigma(u_1^0, p_1^0) \sigma(w_2^\epsilon, \xi_2^\epsilon) dx + \int_{\Omega} \sigma(u_2^0, p_2^0) \sigma(w_1^\epsilon, \xi_1^\epsilon) dx \end{aligned} \quad (20)$$

Combining the variations (18), (19) and (20), we obtain

$$\begin{aligned} \mathcal{J}((u_1^\epsilon, p_1^\epsilon); (u_2^\epsilon, p_2^\epsilon)) - \mathcal{J}((u_1^0, p_1^0); (u_2^0, p_2^0)) &= \int_{\Omega} |\sigma(w_1^\epsilon, \xi_1^\epsilon)|^2 dx + \int_{\Omega} |\sigma(w_2^\epsilon, \xi_2^\epsilon)|^2 dx \\ &\quad - 2 \int_{\Omega} \sigma(w_1^\epsilon, \xi_1^\epsilon) \sigma(w_2^\epsilon, \xi_2^\epsilon) dx + 2 \int_{\Omega} (\sigma(u_1^0, p_1^0) - \sigma(u_2^0, p_2^0)) \sigma(w_1^\epsilon, \xi_1^\epsilon) dx \\ &\quad - 2 \int_{\Omega} (\sigma(u_1^0, p_1^0) - \sigma(u_2^0, p_2^0)) \sigma(w_2^\epsilon, \xi_2^\epsilon) dx. \end{aligned}$$

Therefore,

$$\begin{aligned} \mathcal{J}((u_1^\epsilon, p_1^\epsilon); (u_2^\epsilon, p_2^\epsilon)) - \mathcal{J}((u_1^0, p_1^0); (u_2^0, p_2^0)) - \frac{\partial \mathcal{J}}{\partial u_1}((u_1^0, p_1^0); (u_2^0, p_2^0)) \cdot w_1^\epsilon \\ - \frac{\partial \mathcal{J}}{\partial p_1}((u_1^0, p_1^0); (u_2^0, p_2^0)) \cdot \xi_1^\epsilon - \frac{\partial \mathcal{J}}{\partial u_2}((u_1^0, p_1^0); (u_2^0, p_2^0)) \cdot w_2^\epsilon \\ - \frac{\partial \mathcal{J}}{\partial p_2}((u_1^0, p_1^0); (u_2^0, p_2^0)) \cdot \xi_2^\epsilon = \mathcal{I}(\epsilon), \end{aligned}$$

where

$$\mathcal{I}(\epsilon) = \|\sigma(w_1^\epsilon, \xi_1^\epsilon)\|_{0,\Omega}^2 + \|\sigma(w_2^\epsilon, \xi_2^\epsilon)\|_{0,\Omega}^2 - 2 \int_{\Omega} \sigma(w_1^\epsilon, \xi_1^\epsilon) \sigma(w_2^\epsilon, \xi_2^\epsilon) dx.$$

We will then prove that  $\mathcal{I}(\epsilon) = o(\rho(\epsilon))$ . Thus, the topological asymptotic expansion of the functional  $\mathcal{J}$  with respect to  $\epsilon$  is given by

$$\mathcal{J}(\delta f_\epsilon) - \mathcal{J}(0) = -|\mathcal{S}_{x_0,\epsilon}| \lambda (v_1 + v_2)(x_0) + o(|\mathcal{S}_{x_0,\epsilon}|),$$

then the topological gradient  $\mathcal{G}$  at point  $x_0$  is given by

$$\mathcal{G}(x_0) = -\lambda (v_1 + v_2)(x_0).$$

Let's now show that  $\mathcal{I}(\epsilon) = o(|\mathcal{S}_{x_0,\epsilon}|)$ . Consider  $(w_1^\epsilon, \xi_1^\epsilon) = (u_1^\epsilon - u_1^0, p_1^\epsilon - p_1^0)$  solution of the following problem,

$$\begin{cases} -\operatorname{div}(\sigma(w_1^\epsilon, \xi_1^\epsilon)) &= \delta f_\epsilon & \text{in } \Omega, \\ \operatorname{div} w_1^\epsilon &= 0 & \text{in } \Omega, \\ w_1^\epsilon &= 0 & \text{on } \Gamma_c, \\ \sigma(w_1^\epsilon, \xi_1^\epsilon) n &= 0 & \text{on } \Gamma_i. \end{cases}$$

This problem is well-posed and has a unique solution in  $H^1(\Omega)^d \times L^2(\Omega)$ , see e.g. [7]. Using ([5], theorem 5.2), there exists a positive constant  $C$  such that,

$$\begin{aligned} \|w_1^\epsilon\|_{1,\Omega} + \|\xi_1^\epsilon\|_{0,\Omega} &\leq C \|\delta f_\epsilon\|_{0,\Omega} \\ &\leq C \|\lambda\| (\rho(\epsilon))^{\frac{1}{2}}. \end{aligned} \tag{21}$$

The same for the solution  $(w_2^\epsilon, \xi_2^\epsilon)$ . Using these latter results, we obtain an estimation of the third term of  $\mathcal{I}$ . We deduce then that  $\mathcal{I}(\epsilon) = o(\rho(\epsilon))$ . ■

### 3.3. Identification of the source intensity.

In this subsection, the player (3) assumes to be known the position  $P = x_0$  defining a source-term  $F_\epsilon$  that satisfies (7) and focuses on identifying the source intensity  $\lambda_k$ . To this end, player (3) must minimize the functional  $\mathcal{J}_3$  with respect to  $\lambda$ . So the source intensity can be characterized as the solution of the following minimization problem,

$$\lambda^* = \arg \min_{\lambda \in \mathbb{R}^d} \left\{ \mathcal{J}_3(\eta, \tau; \phi) := \int_{\Omega} |\sigma(u_{1,\epsilon}, p_{1,\epsilon}) - \sigma(u_{2,\epsilon}, p_{2,\epsilon})|^2 dx \right\},$$

where  $(u_{1,\epsilon}, p_{1,\epsilon})$  and  $(u_{2,\epsilon}, p_{2,\epsilon})$  solve respectively problems  $(\mathcal{P}_{1,\epsilon})$  and  $(\mathcal{P}_{2,\epsilon})$ . In order to perform the partial optimization problem of  $\mathcal{J}_3(\eta, \tau; \phi)$  w.r.t the source intensity  $\lambda$  with  $(\eta, \tau)$  given by players (1) and (2), one needs to compute the derivative of  $\mathcal{J}_3$  w.r.t.  $\lambda$ . We have the following:

**Proposition 2.** *We have the following partial derivative,*

$$\frac{\partial \mathcal{J}_3}{\partial \lambda} \cdot \varphi = -\frac{1}{|\mathcal{S}_{x_0,\epsilon}|} \int_{\mathcal{S}_{x_0,\epsilon}} (z_1 + z_2)(x) \cdot \varphi dx, \quad \forall \varphi \in \mathbb{R},$$

where  $(z_1, \pi_1) \in H_{\Gamma_c}^1(\Omega) \times L^2(\Omega)$  and  $(z_2, \pi_2) \in H_{\Gamma_i}^1(\Omega) \times L^2(\Omega)$  are respective solutions of the adjoints problems,

$$\begin{cases} 2 \int_{\Omega} (\sigma(u_{1,\epsilon}, p_{1,\epsilon}) - \sigma(u_{2,\epsilon}, p_{2,\epsilon})) : (\nabla h_1 + \nabla h_1^T) dx - \int_{\Omega} \pi_1 \operatorname{div} h_1 dx \\ \quad + \int_{\Omega} ((\nabla h_1 + \nabla h_1^T) : \nabla z_1) dx = 0, \quad \forall h_1 \in H_{\Gamma_c}^1(\Omega), \\ -2 \int_{\Omega} (\sigma(u_{1,\epsilon}, p_{1,\epsilon}) - \sigma(u_{2,\epsilon}, p_{2,\epsilon})) : (k_1 I_d) dx - \int_{\Omega} k_1 \operatorname{div} z_1 dx = 0, \\ \quad \forall k_1 \in L^2(\Omega), \end{cases} \tag{22}$$

$$\begin{cases} -2 \int_{\Omega} (\sigma(u_{1,\epsilon}, p_{1,\epsilon}) - \sigma(u_{2,\epsilon}, p_{2,\epsilon})) : (\nabla h_2 + \nabla h_2^T) dx - \int_{\Omega} \pi_2 \operatorname{div} h_2 dx \\ \quad + \int_{\Omega} ((\nabla h_2 + \nabla h_2^T) : \nabla z_2) dx = 0, \quad \forall h_2 \in H_{\Gamma_i}^1(\Omega), \\ 2 \int_{\Omega} (\sigma(u_{1,\epsilon}, p_{1,\epsilon}) - \sigma(u_{2,\epsilon}, p_{2,\epsilon})) : (k_2 I_d) dx - \int_{\Omega} k_2 \operatorname{div} z_2 dx = 0, \\ \quad \forall k_2 \in L^2(\Omega), \end{cases} \quad (23)$$

1 and where  $(u_{1,\epsilon}, p_{1,\epsilon})$  and  $(u_{2,\epsilon}, p_{2,\epsilon})$  are the solutions to respectively  $(\mathcal{P}_{1,\epsilon})$  and  $(\mathcal{P}_{2,\epsilon})$ .

### 2 3.4. The three-player Nash algorithm

3 We are now ready to state the three-player identification/completion Nash game. As aforementioned,  
4 players (1) and (2) aim at solving the Cauchy problem, while player (3) is aimed at minimizing a Kohn-  
5 Vogelius type energy, intended to identify the elements of the source-term. The game is of Nash type, which  
6 means that it is static with complete information [17] and hence its solution is a Nash equilibrium (NE), see  
7 Definition 1.

8 Given a triplet  $(\eta, \tau; \phi) \in (H_{00}^{\frac{1}{2}}(\Gamma_i)^d)' \times H^{\frac{1}{2}}(\Gamma_i)^d \times \mathcal{I}_{\text{ad}}$ , and we define  $(u_{1,\epsilon}, p_{1,\epsilon}) := (u_{1,\epsilon}(\eta, \phi), p_{1,\epsilon}(\eta, \phi))$   
9 be the solution to the approximate Stokes problem  $(\mathcal{P}_{1,\epsilon})$  and  $(u_{2,\epsilon}, p_{2,\epsilon}) := (u_{2,\epsilon}(\tau, \phi), p_{2,\epsilon}(\tau, \phi))$  the solution  
10 to the approximate Stokes problem  $(\mathcal{P}_{2,\epsilon})$ , then the three players and their respective costs are defined as  
11 follows:

- Player (1) has control on the Neumann strategies  $\eta \in (H_{00}^{\frac{1}{2}}(\Gamma_i)^d)'$ , and its cost functional is given by

$$\mathcal{J}_1(\eta, \tau; \phi) = \frac{1}{2} \|\sigma(u_{1,\epsilon}, p_{1,\epsilon})n - \Phi\|_{(H_{00}^{\frac{1}{2}}(\Gamma_i)^d)'}^2 + \frac{1}{2} \|u_{1,\epsilon} - u_{2,\epsilon}\|_{H^{\frac{1}{2}}(\Gamma_i)^d}^2. \quad (24)$$

- Player (2) has control on the Dirichlet strategies  $\tau \in H^{\frac{1}{2}}(\Gamma_i)^d$ , and its cost functional is given by

$$\mathcal{J}_2(\eta, \tau; \phi) = \frac{1}{2} \|u_{2,\epsilon} - f\|_{H^{\frac{1}{2}}(\Gamma_i)^d}^2 + \frac{1}{2} \|u_{1,\epsilon} - u_{2,\epsilon}\|_{H^{\frac{1}{2}}(\Gamma_i)^d}^2. \quad (25)$$

- Player (3) has control on the elements  $\phi \in \mathcal{I}_{\text{ad}}$  defining the unknown source, and its cost functional is given by

$$\mathcal{J}_3(\eta, \tau; \phi) = \int_{\Omega} |\sigma(u_{1,\epsilon}, p_{1,\epsilon}) - \sigma(u_{2,\epsilon}, p_{2,\epsilon})|^2 dx. \quad (26)$$

12  
13  
14 Regarding the existence (and uniqueness) issues for the 3-player Nash game stated above, the difficult  
15 access to any nice property of the strongly non-linear map  $\phi \rightarrow \mathcal{J}_3(\eta, \tau; \phi)$  (such as convexity and/or  
16 coerciveness) makes it hard to prove such existence results. When the point-wise sources are known, a much  
17 simpler cas, we successfully tackled the existence and uniqueness issues for the case of missing boundary  
18 data for the Laplace and Stokes equations [17, 18]. We considered two-player Nash game and we introduced  
19 the two functionals  $\mathcal{J}_1$  and  $\mathcal{J}_2$ . These two functionals are quadratic strongly convex with respect to their  
20 specific variables, allowing for a straightforward application of the Nash existence theorem. The uniqueness  
21 is obtained thanks to the *potential structure* of the completion game [17].

22 In Algorithm 1 below, we describe the main steps in computing the Nash equilibrium, with a version  
23 where the Cauchy data of the Dirichlet type  $G$  are possibly perturbed by a noise with some magnitude  $\sigma$ ,  
24 yielding for the Cauchy problem a noisy Dirichlet data  $G^\sigma$ .

25  
26  
27

---

**Algorithm 1:** Computation of the Nash equilibrium  $(\eta_N, \tau_N, \phi_N)$ 


---

**Data:**  $\epsilon_S > 0$  a convergence tolerance,  $K_{max}$  a computational budget per Nash iteration,  $N_{max}$  a maximum Nash iterations and  $\varrho$  tuned-function which depends on the noise magnitude.

Set  $n = 0$ , choose an initial source intensity  $\lambda^{(0)}$  and set  $F_\epsilon = 0$  ;

**while**  $\|u_2 - G\|_{0, \Gamma_c} > \varrho$  **do**

Set  $k = 0$  and choose an initial guess  $(\eta^{(0)}, \tau^{(0)}) \in (H_{00}^{\frac{1}{2}}(\Gamma_i)^d)' \times H^{\frac{1}{2}}(\Gamma_i)^d$  ;

Compute  $\bar{\eta}^{(k)}$  solution of  $\min_{\eta} \mathcal{J}_1(\eta, \tau^{(k)}; F_\epsilon)$ .

Compute (in parallel)  $\bar{\tau}^{(k)}$  solution of  $\min_{\tau} \mathcal{J}_2(\eta^{(k)}, \tau; F_\epsilon)$ .

Evaluate  $(\eta^{(k+1)}, \tau^{(k+1)}) = \alpha(\eta^{(k)}, \tau^{(k)}) + (1 - \alpha)(\bar{\eta}^{(k)}, \bar{\tau}^{(k)})$ , with  $0 \leq \alpha < 1$ .

- **Step I (identify sources locations)** : Set  $F_\epsilon = 0$ , and use the one-shot algorithm to determine the set of optimal locations  $P^{(n)} = \{P_1, \dots, P_{m^{(n)}}\}$ :

- Solve two well-posed mixed forward problems:

$$(\mathcal{P}_1^0) \begin{cases} -\operatorname{div}(\sigma(u_1^{0,k+1}, p_1^{0,k+1})) = 0 & \text{in } \Omega, \\ \operatorname{div} u_1^{0,k+1} = 0 & \text{in } \Omega, \\ u_1^{0,k+1} = G & \text{on } \Gamma_c, \\ \sigma(u_1^{0,k+1}, p_1^{0,k+1})n = \eta^{(k+1)} & \text{on } \Gamma_i, \end{cases}$$

$$(\mathcal{P}_2^0) \begin{cases} -\operatorname{div}(\sigma(u_2^{0,k+1}, p_2^{0,k+1})) = 0 & \text{in } \Omega, \\ \operatorname{div} u_2^{0,k+1} = 0 & \text{in } \Omega, \\ \sigma(u_2^{0,k+1}, p_2^{0,k+1})n = \Phi & \text{on } \Gamma_c, \\ u_2^{0,k+1} = \tau^{(k+1)} & \text{on } \Gamma_i. \end{cases}$$

- Solve the adjoint problems  $(\mathcal{AP}_1)$  and  $(\mathcal{AP}_2)$  with respective solutions  $v_1$  and  $v_2$ .
- Compute the topological gradient  $\mathcal{G}$  using Formula (15), i.e.

$$\mathcal{G}(x) = -\lambda^{(k)} \cdot (v_1 + v_2)(x), \quad \forall x \in \Omega.$$

- Seek

$$P^{(n)} = \arg \min_{x \in \Omega} \mathcal{J}_3(\eta^{(k+1)}, \tau^{(k+1)}; (\lambda^{(k)}, x)).$$

- **Step II (recover boundary data and identify sources magnitudes)**: Solve the Nash game between  $\eta$ ,  $\tau$  and  $\lambda$ : Set  $k = 1$ ,

- Step 1: Set  $F_\epsilon^{(n,k)} = \sum_{i=1}^{m^{(n)}} \frac{1}{|\mathcal{S}_{P_i, \epsilon}|} \lambda_i^{(k-1)} \chi_{\mathcal{S}_{P_i, \epsilon}}$ .
- Step 2: Compute  $\bar{\eta}^{(k)}$  solution of  $\min_{\eta} \mathcal{J}_1(\eta, \tau^{(k)}; (\lambda^{(k-1)}, P^{(n)}))$ .
- Step 3: Compute (in parallel)  $\bar{\tau}^{(k)}$  solution of  $\min_{\tau} \mathcal{J}_2(\eta^{(k)}, \tau; (\lambda^{(k-1)}, P^{(n)}))$ .
- Step 4: Compute (in parallel)  $\bar{\lambda}^{(k)}$  solution of  $\min_{\lambda} \mathcal{J}_3(\eta^{(k)}, \tau^{(k)}; (\lambda, P^{(n)}))$ .
- Step 5: For  $0 \leq \alpha < 1$ , set

$$S^{(k+1)} = (\eta^{(k+1)}, \tau^{(k+1)}, \lambda^{(k)}) = \alpha(\eta^{(k)}, \tau^{(k)}, \lambda^{(k-1)}) + (1 - \alpha)(\bar{\eta}^{(k)}, \bar{\tau}^{(k)}, \bar{\lambda}^{(k)}).$$

While  $\|S^{(k+1)} - S^{(k)}\| > \epsilon_S$  and  $k < N_{max}$ , set  $k = k + 1$ , return back to step 1.

**end**

---

1 The topological gradient and the gradient with fixed step methods are used to solve step I and II,  
2 respectively, in Algorithm 1. In step II, in order to solve the problems of partial optimization of  $\mathcal{J}_1$ ,  $\mathcal{J}_2$  and  
3  $\mathcal{J}_3$ , we need to calculate the gradient of these costs with respect to their respective strategies  $\eta$ ,  $\tau$  and  $\lambda$ .  
4 The fast computation of the latter is classical, and led by means of an adjoint state method, as shown by  
5 the proposition 2 and 3, the proof of the proposition 3 is given in ([18], Appendix A. 1).

6 **Proposition 3.** [18] *We have the following two partial derivatives:*

$$\left\{ \begin{array}{l} \frac{\partial \mathcal{J}_1}{\partial \eta} \cdot \psi = - \int_{\Gamma_i} \psi \lambda_1 ds, \quad \forall \psi \in (H_{00}^{\frac{1}{2}}(\Gamma_i)^d)', \\ \text{with } (\lambda_1, \kappa_1) \in H_{\Gamma_c}^1(\Omega) \times L^2(\Omega) \text{ solution of the adjoint problem:} \\ \left\{ \begin{array}{l} \int_{\Gamma_c} (\sigma(u_{1,\epsilon}, p_{1,\epsilon})n - \Phi)((\nabla \gamma + \nabla \gamma^T)n) ds + \int_{\Gamma_i} (u_{1,\epsilon} - u_{2,\epsilon})\gamma ds \\ \quad + \int_{\Omega} (\nabla \gamma + \nabla \gamma^T) : \nabla \lambda_1 dx - \int_{\Omega} \kappa_1 \operatorname{div} \gamma dx = 0, \quad \forall \gamma \in H_{\Gamma_c}^1(\Omega), \\ - \int_{\Gamma_c} (\sigma(u_{1,\epsilon}, p_{1,\epsilon})n - \Phi)\delta n ds - \int_{\Omega} \delta \operatorname{div} \lambda_1 dx = 0, \quad \forall \delta \in L^2(\Omega), \end{array} \right. \end{array} \right. \quad (27)$$

$$\left\{ \begin{array}{l} \frac{\partial \mathcal{J}_2}{\partial \tau} \cdot \mu = \int_{\Gamma_i} (\sigma(\lambda_2, \kappa_2)n - (u_{1,\epsilon} - u_{2,\epsilon}))\mu ds, \quad \forall \mu \in H^{\frac{1}{2}}(\Gamma_i)^d, \\ \text{with } (\lambda_2, \kappa_2) \in H^1(\Omega)^d \times L^2(\Omega) \text{ solution of the adjoint problem:} \\ \left\{ \begin{array}{l} \int_{\Omega} (\nabla \lambda_2 + \nabla \lambda_2^T) : \nabla \varphi dx - \int_{\Omega} \kappa_2 \operatorname{div} \varphi dx = \int_{\Gamma_c} (G - u_{2,\epsilon})\varphi ds, \\ \quad \forall \varphi \in H_{\Gamma_i}^1(\Omega), \\ \int_{\Omega} \xi \operatorname{div} \lambda_2 dx = 0, \quad \forall \xi \in L^2(\Omega), \end{array} \right. \end{array} \right. \quad (28)$$

7 where, by a classical convention,  $\nabla u : \nabla v = \operatorname{Tr}(\nabla u \nabla v^T) = \sum_{i,j} \frac{\partial u_i}{\partial x_j} \frac{\partial v_i}{\partial x_j}$ .

9 Algorithm 1 is made of an overall while-do loop which assesses the global convergence based on the  
10 identifiability result stated in Theorem-1, and whose computational cost is controlled by  $N_{max}$ .

11 The task **Step I (identify sources locations)** costs solving 4 problems by Finite Element Method (FEM),  
12 while computing the topological gradient has a negligible cost, as well as is finding the optimal locations  
13 since it only amounts to ordering of the significantly negative components of the topological gradient.

14 The task **Step II (recover boundary data and identify sources magnitudes)** costs 3 optimizations em-  
15 bedded in a **data completion** while-do loop again controlled by  $N_{max}$ .

16 Minimizations in Step 2 and Step 3 costs each  $4 \times NC$  FEM solving where  $NC$  is the total number of degrees  
17 of freedom of the  $\Gamma_i$  boundary nodes : we solve for 2 direct Stokes problems, and 2 adjoint Stokes problems  
18 at each minimization iteration, and we use either fixed or conjugate gradient methods since the costs are  
19 quadratic with respect to the controls. The cost of the minimization in Step 4 is relatively negligible thanks  
20 to the quadratic dependence of the cost  $\mathcal{J}_3$  with respect to the magnitudes.

## 21 4. Numerical experiments

22 In this section, we illustrate the numerical results obtained using the 3-costs functionals described in the  
23 previous section 3. In order to test the efficiency of the proposed numerical method, we solve the source  
24 Cauchy-Stokes problem in the 2-D situations: the annular domain and a geometry with corners are consid-  
25 ered. Then, we present an example of numerical reconstruction in the three-dimensional 3-D case. In our  
26 numerical experiments, we use L2 norms to estimate errors and calculate the gradient of the cost functionals.

27  
28 Given a known the elements defining the source term  $F_\epsilon^*$ , that is  $\phi^* = (\lambda, P)$ , we solve the following  
29 Stokes problem :



$$\begin{cases} -\operatorname{div}(\sigma(u, p)) = F_\epsilon^* & \text{in } \Omega, \\ \operatorname{div} u = 0 & \text{in } \Omega, \\ u = G & \text{on } \Gamma_c, \\ \beta u + \gamma \sigma(u, p)n = \beta H + \gamma \Psi & \text{on } \Gamma_i, \end{cases} \quad (29)$$

1 where the (phantom) exact solution  $(u, p)$  is used to build the remaining Cauchy data  $\Phi = \sigma(u, p)n|_{\Gamma_c}$ , and  
2 the exact missing data  $u|_{\Gamma_i}$  and  $\sigma(u, p)n|_{\Gamma_i}$ . The two latter data together with the known elements defining  
3  $F_\epsilon^*$  are used to compute the following relative errors :

$$\begin{aligned} err_D &= \frac{\|\tau_N - u|_{\Gamma_i}\|_{0, \Gamma_i}}{\|u|_{\Gamma_i}\|_{0, \Gamma_i}}, & err_N &= \frac{\|\eta_N - \sigma(u, p)n|_{\Gamma_i}\|_{0, \Gamma_i}}{\|\sigma(u, p)n|_{\Gamma_i}\|_{0, \Gamma_i}}, \\ err_P &= \frac{\|P_{ex} - P_{op}\|_2}{\|P_{ex}\|_2}, & err_\lambda &= \frac{\|\Lambda_{ex} - \Lambda_{op}\|_2}{\|\Lambda_{ex}\|_2}, \end{aligned} \quad (30)$$

4 where  $(\eta_N, \tau_N; \phi_N)$  is the approximate Nash equilibrium output from Algorithm 1, and  $\|\cdot\|_2$  represents the  
5 Euclidean norm. These metrics are used to assess the efficiency of our approach. The stability w.r.t. noise  
6 was stressed by solving the coupled problem with noisy perturbations of the Dirichlet data  $G^\sigma = G(1 + \sigma\delta)$ ,  
7 with  $\delta$  is a random real number taken from the uniform distribution over the interval  $[-1, 1]$ .

8 An arbitrary initial guess such as  $S^{(0)} = (\eta^{(0)}, \tau^{(0)}, \lambda^{(0)}) = (0, 0, 0.1)$  and  $F_\epsilon = 0$  are chosen to start the  
9 algorithm, and the relaxation parameter  $\alpha$  is set to 0.25. The pointwise forces identified are represented in  
10 the domain  $\Omega$  as a disc of radius  $\epsilon = 0.07$ .

11 The solvers for Stokes, the computation of the topological gradient and adjoint systems, and the mini-  
12 mization algorithms as well, were implemented using the Finite Element package FreeFem++ [20].

13 *Example 1: An annular domain.*

14  
15 We consider an annular domain  $\Omega$  with circular boundary components  $\Gamma_i$  and  $\Gamma_c$ , both centered at  $(0, 0)$   
16 and with radii  $R_i = 1$  and  $R_c = 2$ , respectively. In this example, we choose  $(\beta, \gamma) = (0, 1)$ , and the Cauchy  
17 data  $\sigma(u, p)n|_{\Gamma_c}$  is generated via the solution of the problem (4), with  $G|_{\Gamma_c} = (y^2, x^2)$  and  $\Psi|_{\Gamma_i} = -(x, y)$ .

18 *Test-case A.*

19 The exact source-term is located at  $P_{ex} = (1.8, 0)$ , with an intensity source  $\Lambda_{ex} = (0.2, 0.2)$ .

20  
21 We applied our algorithm 1, presented in section 3, to compute the Nash equilibrium. Figure 5 presents  
22 the obtained results. We remark that these results are in good accordance with the exact source  $F_\epsilon$  and  
23 missing data.

24 For the case of noisy Dirichlet data  $G^\sigma$  given over  $\Gamma_c$ , it can be seen from the profiles presented in Figure  
25 6 and the Table 4 that the boundary data recovery is overall stable with respect to the noise magnitude, in  
26 particular the computed components of the normal stress are more sensitive than the velocity one, and the  
27 estimated elements defining  $F_\epsilon$ , identified source and their intensity forces, are also acceptable.

28 The relative errors defined by formulas (30) are summarized in Table 1 for the test-case A.

29

Table 1: Test-case A.  $L^2$  relative errors on missing data on  $\Gamma_i$  (on Dirichlet and Neumann data), and the relative errors on the identified source position and on the identified source intensity for various noise levels.

Noise level	$err_D$	$err_N$	$err_P$	$err_\Lambda$
$\sigma = 0\%$	0.003	0.060	0.010	0.018
$\sigma = 1\%$	0.008	0.087	0.010	0.155
$\sigma = 3\%$	0.015	0.147	0.043	0.169

1 *Test-case B. The case of multiple points-forces.*

2  
3 In this test-case, we try to detect and locate multiple point-forces. We propose to identify four pointwise  
4 forces, located respective at the points  $P_1 = (1.8, 0)$ ,  $P_2 = (0, 1.8)$ ,  $P_3 = (-1.8, 0)$  and  $P_4 = (0, -1.8)$ , and  
5 their exact intensity force  $\lambda_i$  is equal to  $(0.2, 0.2)$ ,  $i=1, \dots, 4$ .

6  
7 We suppose that the number  $m$  of the region  $\mathcal{S}_{P_i, \epsilon}$ ,  $i=1, \dots, m$ , is unknown. We observe from Figure 7(a)(b)  
8 that our proposed algorithm is able to determine the number of the small region inside  $\Omega$  and gives a good  
9 approximation of the locations and the recovery intensity for each components of the source-term, as well  
10 as the recovered data Figure 7(c)-(f). The recovery of missing boundary data and the estimated value of  $P$   
11 and  $\lambda$  are stable with respect to noisy Dirichlet measurements, as shown Figure 8 and Table 5, where the  
12 table 5 presents the different error at convergence.

13 To assess our algorithm and results against the so-called inverse crime, that possibly arises when the  
14 same model is used to synthesize Cauchy data and to solve the corresponding inverse problem, resulting in  
15 possible artificial outperformance, we synthesized Cauchy data using different meshes, see Figure 2. All our  
16 numerical experiments produced results of the same good quality than the results presented in Figure 7, see  
17 Figure 9.

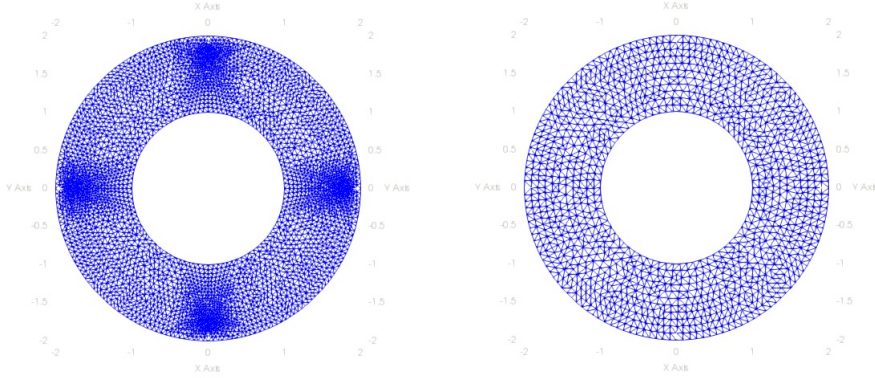


Figure 2: Test case B. (Left) Mesh used for solving the direct problem, in order to construct the synthetic data. (Right) Mesh used for solving the coupled inverse problem, with P2-P1 finite element.

18 *Example 2: A geometry with corners.*

19 The domain is a centered square  $] -0.5, 0.5[ \times ] -0.5, 0.5[$ , the finite element discretization of the domain  
20 boundary  $\partial\Omega$  is constituted of 160 vertices. We impose here  $(\beta, \gamma) = (1, 0)$ , and  $G = H = (2y^2 - 1/2, 0)$   
21 prescribed over  $\partial\Omega$ .

22 Overspecified Cauchy data are prescribed on the boundaries  $y \in \{-\frac{1}{2}, \frac{1}{2}\}$  and  $x = -1/2$  of the square and  
23 the underspecified boundary data  $u|_{\Gamma_i} = u(1/2, y)$  and its stress force are sought.

24 *Test-case C.*

25 The exact source-term is located at  $P_{ex} = (-0.3, -0.25)$ , with intensity  $\Lambda_{ex} = (0.25, 0.2)$ .

26  
27 The numerically obtained results are shown in Figure 10. Figure 10(a) presents the iso-values of the  
28 topological gradient, the source support  $\mathcal{S}_{x_0, \epsilon}$  can be located in the areas where the topological gradient is  
29 negative. The estimated intensity and the determined position are very satisfactory, as shown Figure 10(b).  
30 The numerical Dirichlet solution is a good approximation for the exact solution one, see Figure 10(c)(d).  
31 Then, concerning the numerical Neumann solution, see Figure 10(e)(f), it can be seen that the estimates

1 deviate from the exact one, especially near the endpoints of the boundary which is the region of singularities,  
 2 in the corners. There is also a remarkable stability with respect to noisy data of both the estimated elements  
 3 and the recovered boundary data, see Figure 11 and Table 6.

4 The relative errors presented in Table 2 show the performance of our method with respect to noisy  
 5 Dirichlet measurements.

Table 2: Test-case C.  $L^2$  relative errors on missing data on  $\Gamma_i$  (on Dirichlet and Neumann data), and the relative errors on the identified source position and on the identified source intensity for various noise levels.

Noise level	$err_D$	$err_N$	$err_P$	$err_\Lambda$
$\sigma = 0\%$	0.011	0.097	0.071	0.009
$\sigma = 1\%$	0.011	0.102	0.136	0.029
$\sigma = 3\%$	0.021	0.106	0.184	0.058

6 A numerical study concerning the sensitivity of the reconstruction according to the position of the source  
 7 term in the domain has been studied. The Figure 3 shows that the relative errors increase when the source  
 8 term becomes closer to the inaccessible boundary  $\Gamma_i$ .

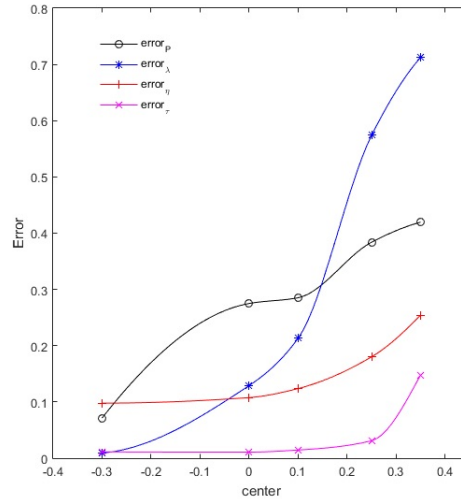


Figure 3: Test case C. Sensitivity of the reconstruction w.r.t. the distance to the inaccessible boundary  $\Gamma_i$ , the distance of the center of  $\mathcal{S}_{P,\epsilon}$  from  $\Gamma_i$ , for  $y = -0.25$ .

### 9 The 3D case.

10 We present hereafter an example of numerical reconstruction in the three dimensional case. The domain  
 11  $\Omega$  is a cube  $(0, 1)^3$ , such that its boundary splitted into two parts  $\Gamma_i$  and  $\Gamma_c$ , where  $\Gamma_i = \{(x, y, z) \in$   
 12  $\partial\Omega; \text{ such that } x = 1\}$  represents the inaccessible part and  $\Gamma_c = \partial\Omega \setminus \Gamma_i$  is the accessible part, where the  
 13 Cauchy data is available. We try so to detect a source  $F_\epsilon$  located in  $P_{ex} = (0.25, 0.25, 0.25)$  and with a source  
 14 intensity  $\lambda_{ex} = (0.25, 0.2, 0)$ . The Cauchy data on  $\Gamma_c$  are numerically simulated by solving the following  
 15 Dirichlet problem:

$$\begin{cases} -\operatorname{div}(\sigma(u, p)) &= F_\epsilon^* & \text{in } \Omega, \\ \operatorname{div} u &= 0 & \text{in } \Omega, \\ u &= G & \text{on } \partial\Omega, \end{cases}$$

1 where  $G$  is a given function. Then, applying our algorithm 1 in order to find the Nash equilibrium, which  
 2 is expected to approximate the coupled problem solution. The finite element computations are performed  
 3 with 4,096 nodes and 20,250 tetrahedral elements. The cost of computation is quite expensive, to overcome  
 4 this difficulty, we use `ffdm` which implements a class of parallel solvers in FreeFem. The obtained results  
 5 are presented in Table 3, with noise free Dirichlet data over  $\Gamma_c$ . The Figure 4 represents the iso-values of the  
 6 topological gradient at convergence.

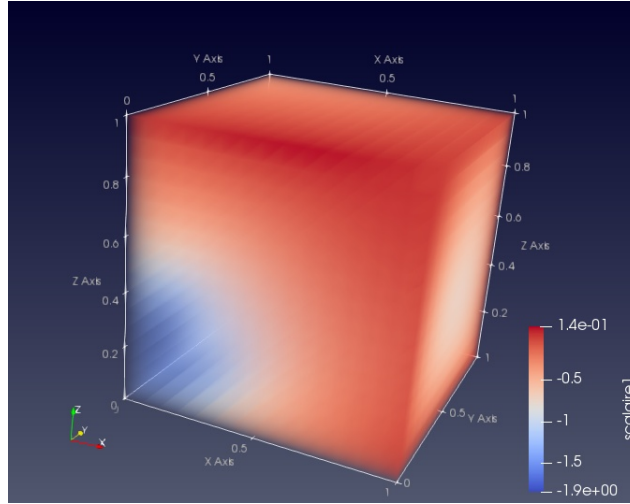


Figure 4: The iso-values of the topological gradient at convergence,  $P_{op} = (0.2, 0.2, 0.2)$  and  $\Lambda_{op} = (0.233, 0.204, 0.005)$ . Exact values:  $P_{ex} = (0.25, 0.25, 0.25)$  and  $\Lambda_{ex} = (0.25, 0.2, 0)$ .

Table 3:  $L^2$  relative errors of reconstructed solution in the whole domain and missing data on  $\Gamma_i$  (on Dirichlet and Neumann data), and the relative errors on the identified source position and on the identified source intensity for noise-free, where  $err_{u_i} = \|u_{i,\epsilon} - u\|_{0,\Omega} / \|u\|_{0,\Omega}$ , for  $i = 1, 2$ .

$err_{u_1}$	$err_{u_2}$	$err_{\tau}$	$err_{\eta}$	$err_P$	$err_{\Lambda}$
0.008	0.026	0.031	0.224	0.2	0.056

## 7 5. Conclusion

8 we have addressed, in the present paper, the problem of identifying the location and magnitude of a finite  
 9 but unknown number of point-wise sources, in a linear steady Stokes problem with missing boundary data.  
 10 Such a reconstruction problem couples two inverse problems of different classes, the recovery of missing  
 11 boundary data (the Cauchy problem), and the identification of point-wise sources. Each of these two  
 12 inverse problems is known to be severely ill-posed by its own, and designing efficient and stable algorithms  
 13 is challenging. In our case, the problem of designing efficient and robust algorithms is worsened by the  
 14 coupling of the two ill-posed problems, and by the fact that we consider as available only a single pair of  
 15 over-specified data (and not the classical Dirichlet-to-Neumann whole map).

16 Due to the identification/recovery coupling, classical methods fail, mainly because of being too specific  
 17 to each of the source identification or data recovery problems. Hence our recourse to game theory, which  
 18 is, by its very nature, able to address such antagonistic situations. Previous successful reframing of data  
 19 recovery inverse problems as Nash games has fostered the formulation of the coupled source identification  
 20 and data recovery problems as Nash games.

1 We have proposed here to formulate the coupled inverse problems as a static with complete information  
2 Nash game. First, we have relaxed the point-wise source identification problem to gain some regularity on  
3 the velocity and pressure state variables, and we have introduced three players and three cost functionals.  
4 The two first, named Dirichlet-Neumann players, were dedicated to ensure the data completion while the  
5 third one was dedicated to ensure the detection of the sources. We postulated that the sought solution of  
6 the coupled problem could be found as a Nash equilibrium of the three-player game.

7 This formulation resulted in the design of a novel algorithm, which is composed of two main steps. In  
8 the first step, the third player seeks to identify the number and location of the sources using a topological  
9 gradient method. In the second one, the two Dirichlet-Neumann players solve the data completion, in a  
10 parallel task with the third player, which minimizes a Kohn-Vogelius like functional in order to identify the  
11 different sources magnitudes.

12 The efficiency and robustness of our coupled reconstruction algorithm was proved against several numer-  
13 ical experiments led for different two- and three-dimensional test-cases.

14 *Acknowledgments.* This work was financially supported by the PHC Utique program NAMRED of the  
15 French Ministry of Foreign Affairs and Ministry of higher education, research and innovation and the Tunisian  
16 Ministry of higher education and scientific research in the CMCU project number 18G1502.

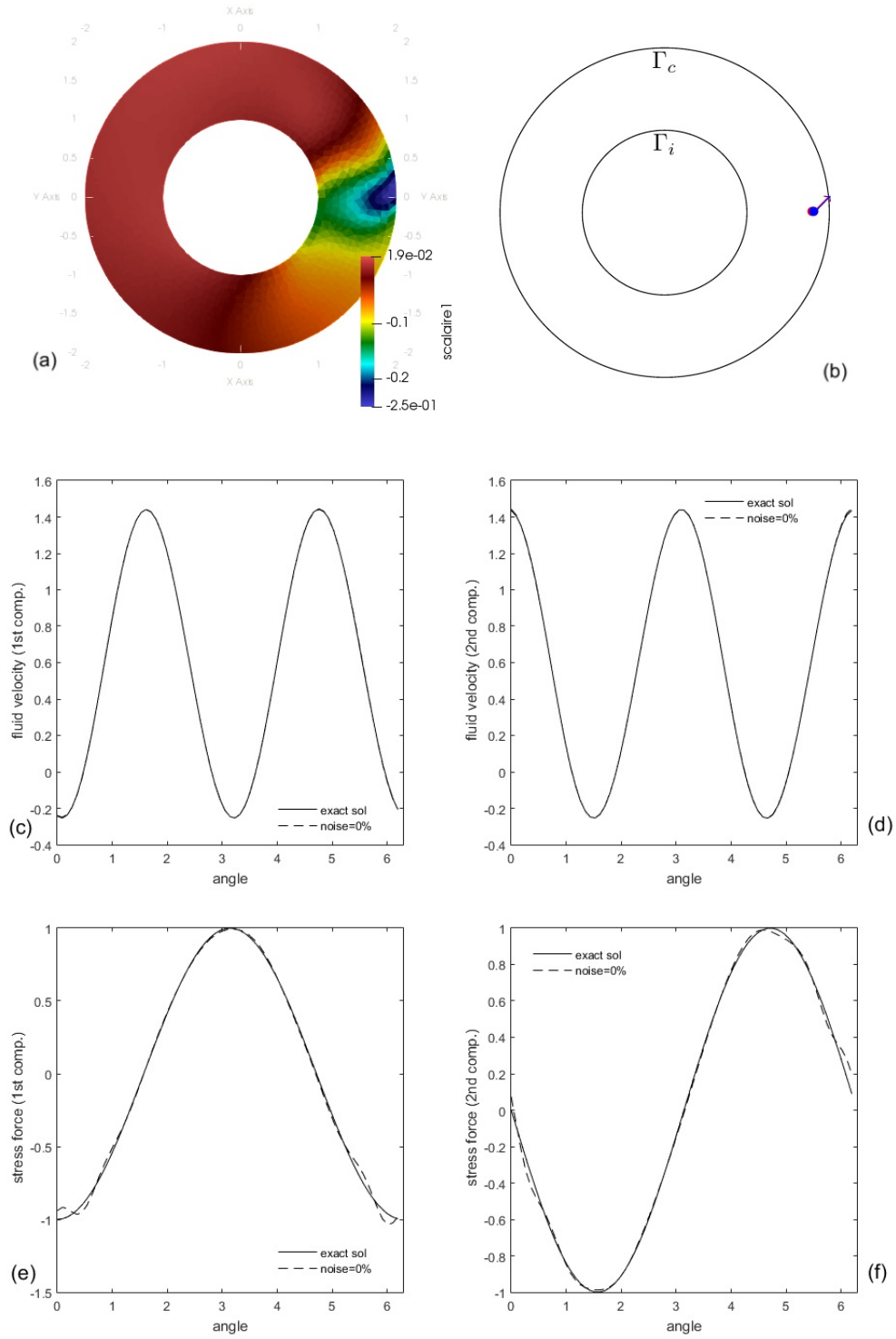


Figure 5: Test case A. Reconstruction of the point-forces and missing boundary data with noise free Dirichlet data over  $\Gamma_c$ . (a) the iso-values of the topological gradient at convergence. (b) exact elements defining the source-term -red vector- and computed one -blue vector- (c) exact -line- and computed -dashed line- first component of the velocity over  $\Gamma_i$ . (d) exact -line- and computed -dashed line- second component of the velocity over  $\Gamma_i$ . (e) exact -line- and computed -dashed line- first component of the normal stress over  $\Gamma_i$  (f) exact -line- and computed -dashed line- second component of the normal stress over  $\Gamma_i$ .

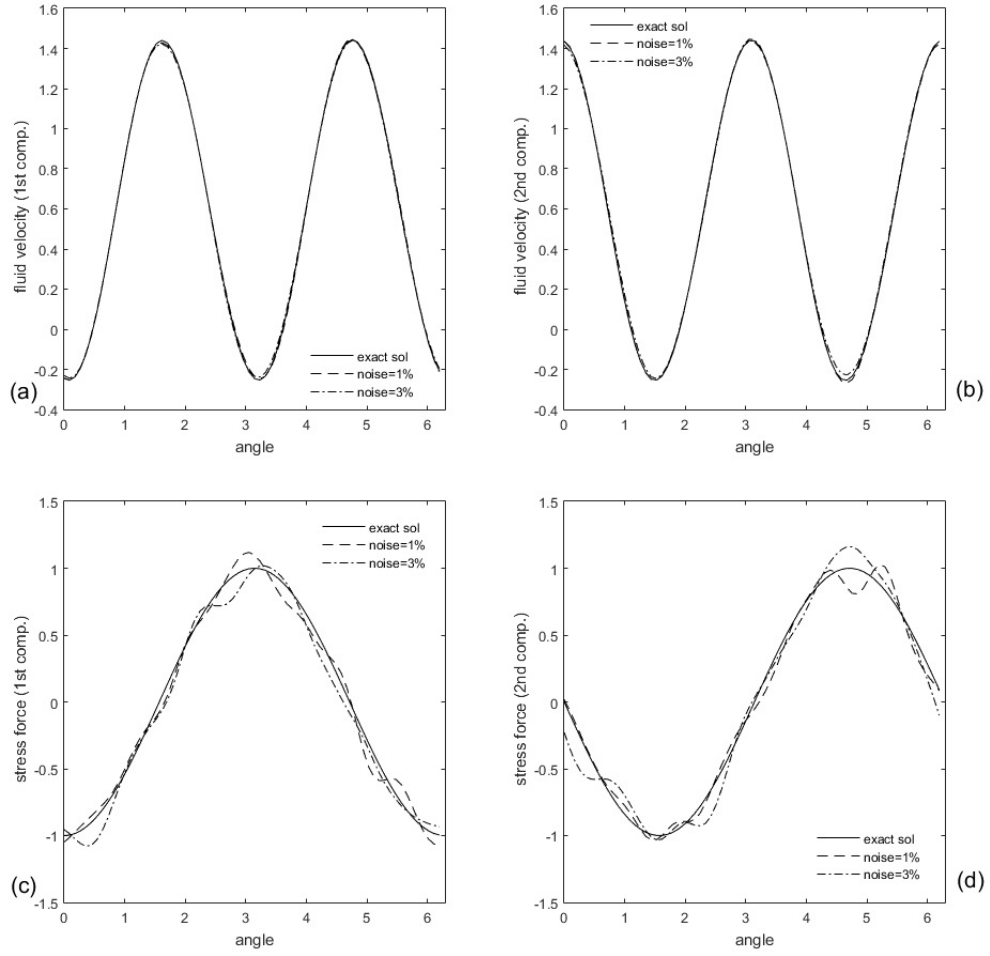


Figure 6: Test case A. Reconstruction of the missing boundary data with noisy Dirichlet data over  $\Gamma_c$  with noise levels  $\sigma = \{1\%, 3\%\}$ . **(a)** exact and computed first components of the velocity over  $\Gamma_i$  **(b)** exact and computed second components of the velocity over  $\Gamma_i$  **(c)** exact and computed first components of the normal stress over  $\Gamma_i$  **(d)** exact and computed second components of the normal stress over  $\Gamma_i$ .

Table 4: Test-case A. Identified source position and their intensity for various noise levels.

Noise level	$\sigma = 0\%$	$\sigma = 1\%$	$\sigma = 3\%$	
$P_{op}$	(1.81,-2e-09)	(1.81,-2.e-09)	(1.84,-0.066)	$P_{ex} = (1.8, 0)$
$\Lambda_{op}$	(0.195,0.202)	(0.161,0.179)	(0.2,0.152)	$\Lambda_{ex} = (0.2, 0.2)$

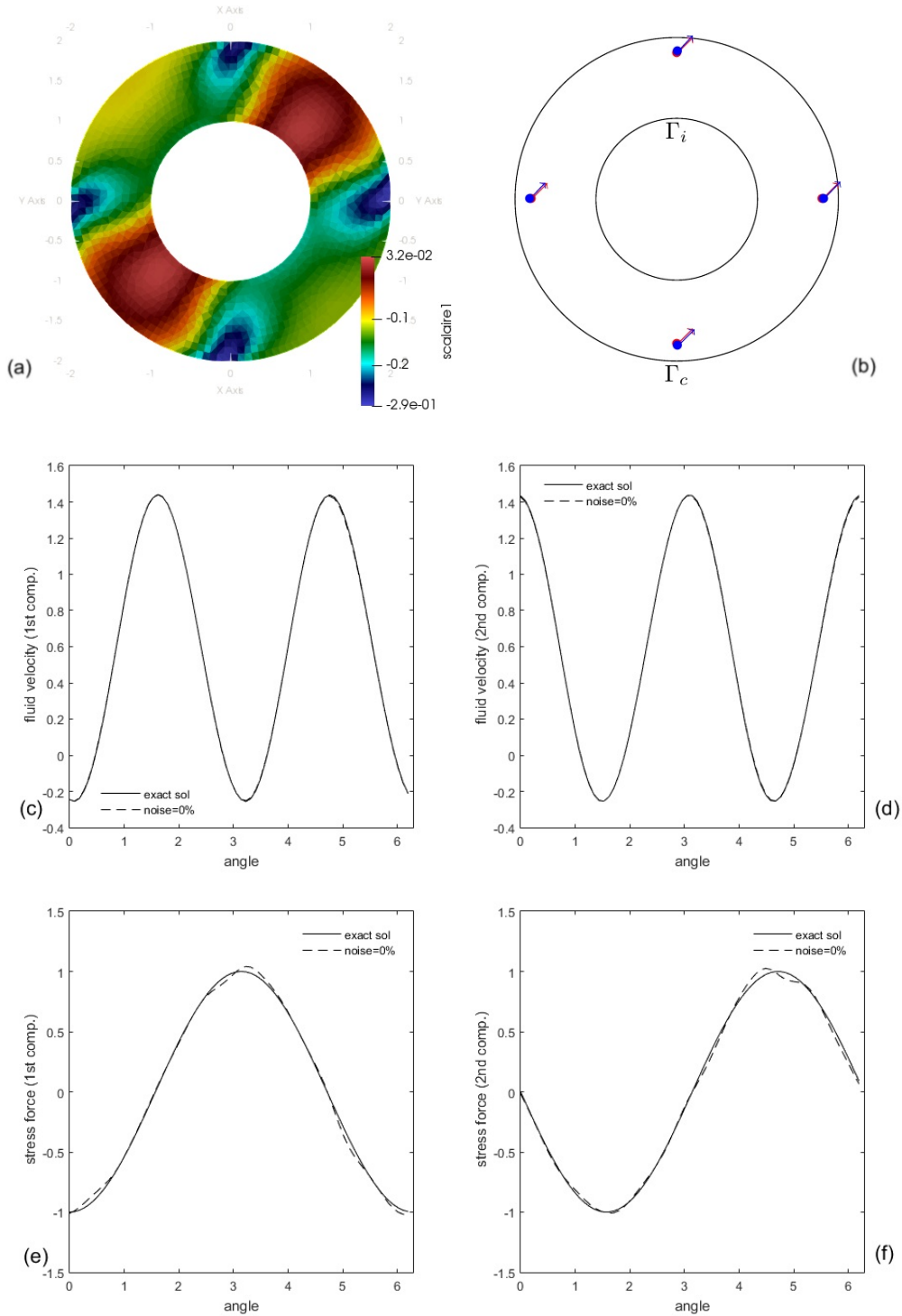


Figure 7: Test case B. Reconstruction of the point-forces and missing boundary data with noise free Dirichlet data over  $\Gamma_c$ . (a) the iso-values of the topological gradient at convergence. (b) exact elements defining the source-term -red vector- and computed one -blue vector- (c) exact -line- and computed -dashed line- first component of the velocity over  $\Gamma_i$ . (d) exact -line- and computed -dashed line- second component of the velocity over  $\Gamma_i$ . (e) exact -line- and computed -dashed line- first component of the normal stress over  $\Gamma_i$ . (f) exact -line- and computed -dashed line- second component of the normal stress over  $\Gamma_i$ .



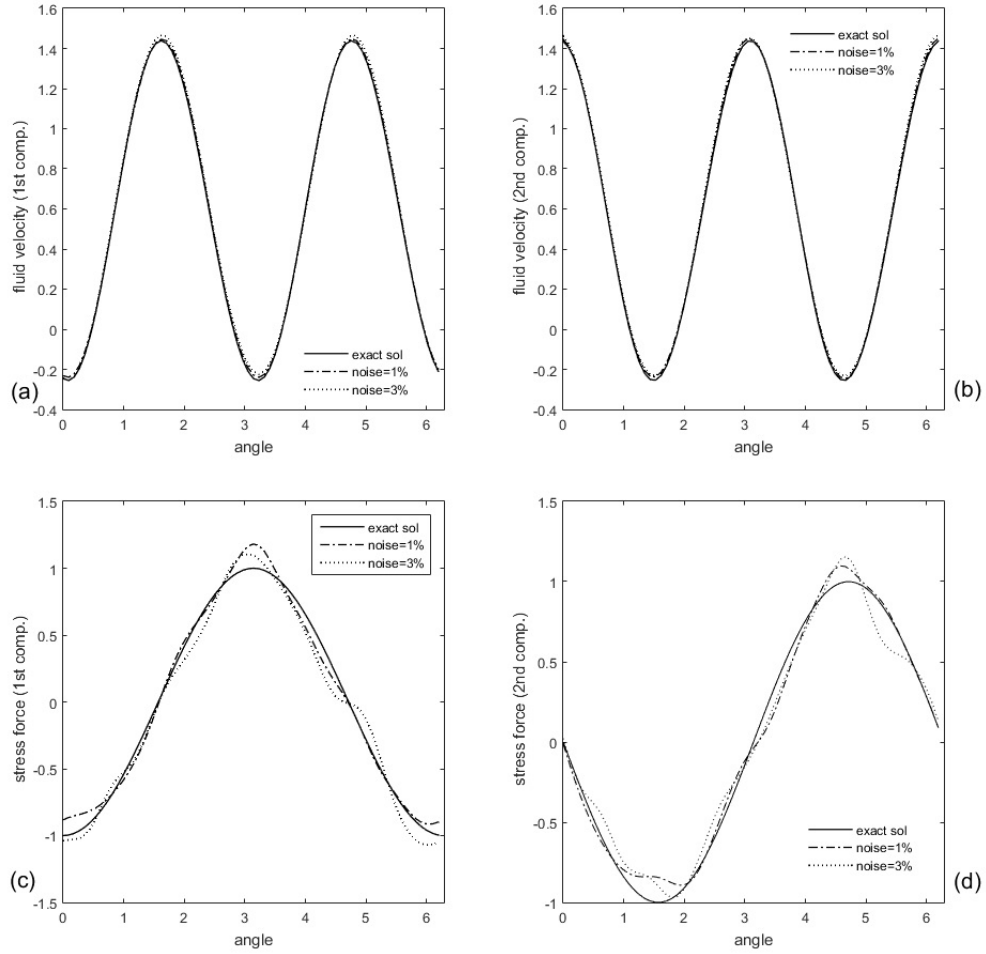


Figure 8: Test case B. Reconstruction of the missing boundary data with noisy Dirichlet data over  $\Gamma_c$  with noise levels  $\sigma = \{1\%, 3\%\}$ . (a) exact and computed first components of the velocity over  $\Gamma_i$  (b) exact and computed second components of the velocity over  $\Gamma_i$  (c) exact and computed first components of the normal stress over  $\Gamma_i$  (d) exact and computed second components of the normal stress over  $\Gamma_i$ .

Table 5: Test-case B.  $L^2$  relative errors on missing data on  $\Gamma_i$  (on Dirichlet and Neumann data), and the relative errors on the identified source position and on the identified source intensity for various noise levels.

Noise level	$err_D$	$err_N$	$err_P$	$err_\Lambda$
$\sigma = 0\%$	0.005	0.056	0.010	0.049
$\sigma = 1\%$	0.013	0.113	0.010	0.181
$\sigma = 3\%$	0.025	0.141	0.043	0.24

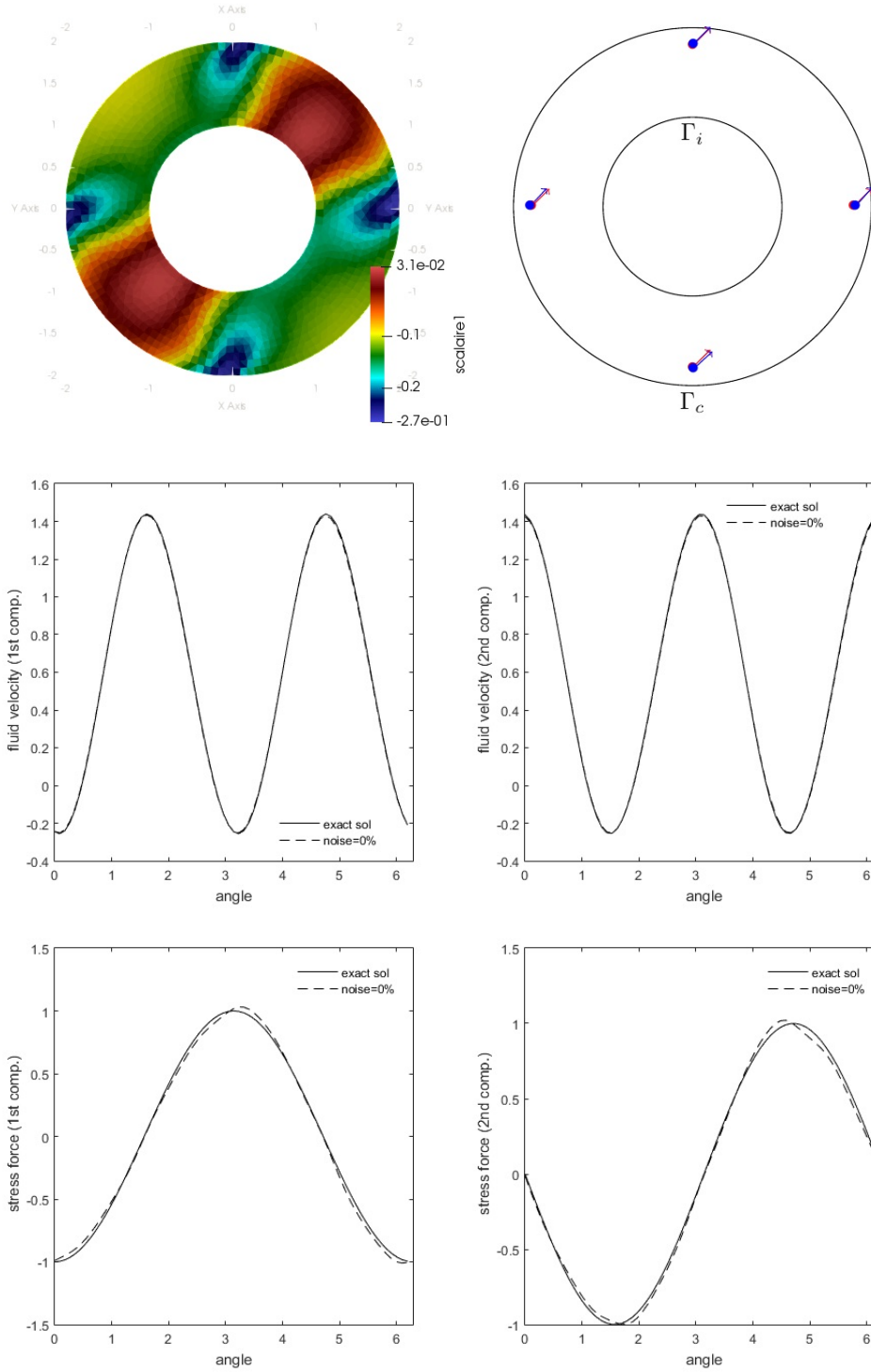


Figure 9: Test case B: Assessing Inverse-Crime-Free reconstruction. Test case B. Top: the iso-values of the topological gradient at convergence, and the exact and optimal elements defining the source-term. Middle: the two components of the velocity on  $\Gamma_i$ . Bottom: the two components of the normal stress on  $\Gamma_i$  ( $err_\tau = 0.00768152$ ,  $err_\eta = 0.0713575$ ,  $err_P = 0.0105486$ , and  $err_\Lambda = 0.0560551$ ).

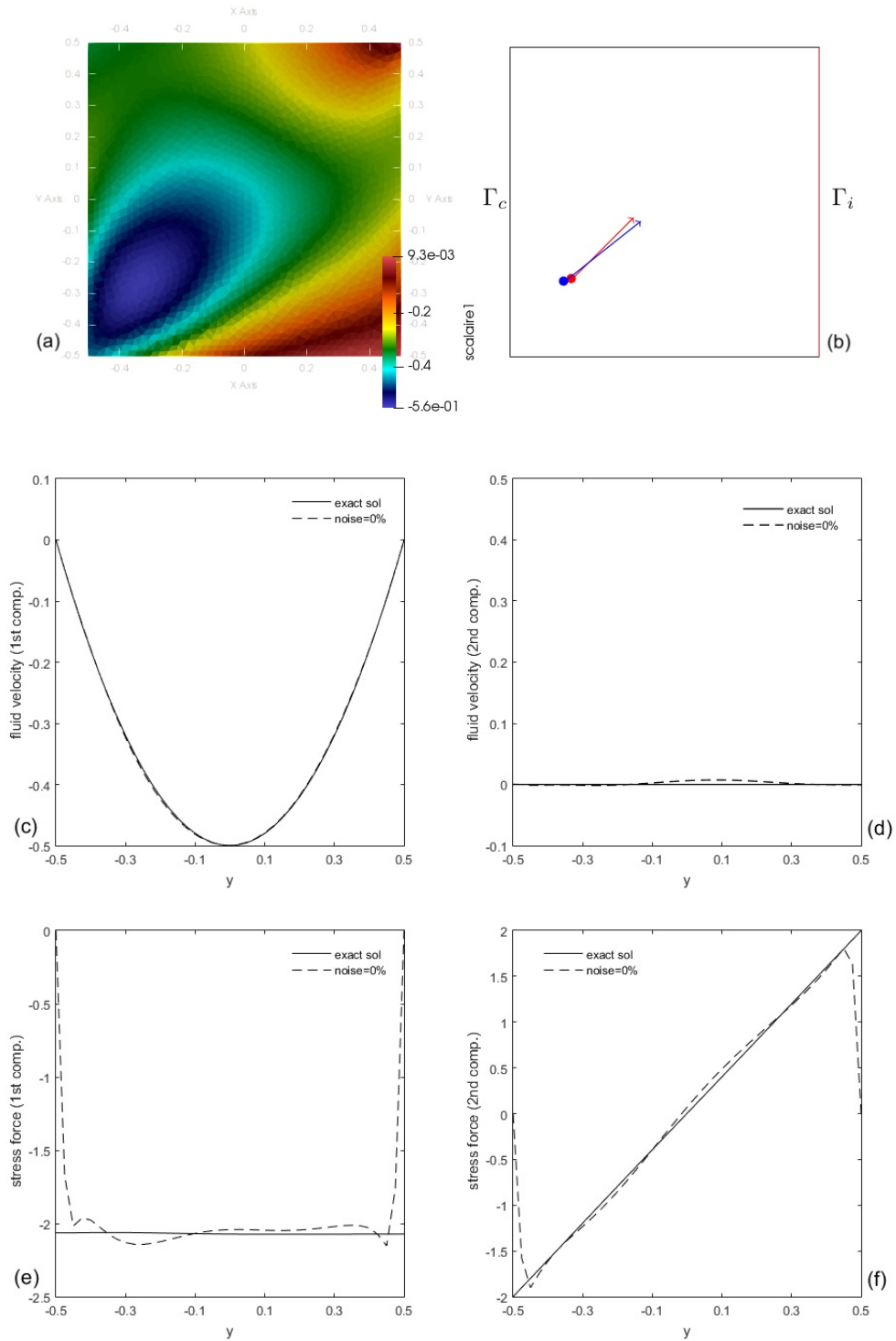


Figure 10: Test case C. Reconstruction of the point-forces and missing boundary data with noise free Dirichlet data over  $\Gamma_c$ . (a) the iso-values of the topological gradient at convergence. (b) exact elements defining the source-term -red vector- and computed one -blue vector- (c) exact -line- and computed -dashed line- first component of the velocity over  $\Gamma_i$ . (d) exact -line- and computed -dashed line- second component of the velocity over  $\Gamma_i$ . (e) exact -line- and computed -dashed line- first component of the normal stress over  $\Gamma_i$  (f) exact -line- and computed -dashed line- second component of the normal stress over  $\Gamma_i$ .

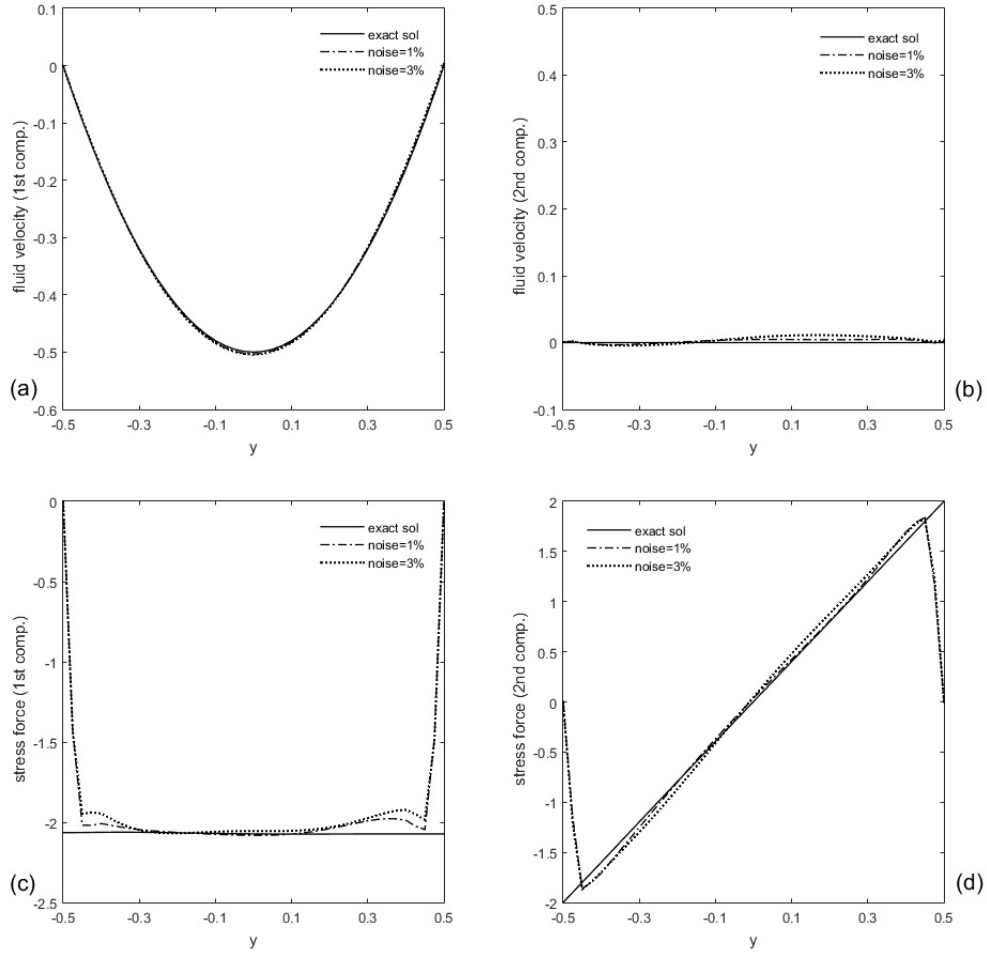


Figure 11: Test case C. Reconstruction of the missing boundary data with noisy Dirichlet data over  $\Gamma_c$  with noise levels  $\sigma = \{1\%, 3\%\}$ . (a) exact and computed first components of the velocity over  $\Gamma_i$  (b) exact and computed second components of the velocity over  $\Gamma_i$  (c) exact and computed first components of the normal stress over  $\Gamma_i$  (d) exact and computed second components of the normal stress over  $\Gamma_i$ .

Table 6: Test-case C. Identified source position and their intensity for various noise levels.

Noise level	$\sigma = 0\%$	$\sigma = 1\%$	$\sigma = 3\%$	
$P_{op}$	(-0.326,-0.259)	(-0.339,-0.285)	(-0.36,-0.29)	$P_{ex} = (-0.3, -0.25)$
$\Lambda_{op}$	(0.248,0.197)	(0.24,0.199)	(0.231, 0.196)	$\Lambda_{ex} = (0.25, 0.2)$

## 1 References

## 2 References

- 3 [1] R. Aboulaich, A. Ben Abda, and M. Kallel. A control type method for solving the Cauchy-Stokes problem. *Applied*
- 4 *Mathematical Modelling*, 37:4295–4304, 2013.
- 5 [2] A. Allendes, E. Otárola, and A. J. Salgado. A posteriori error estimates for the stokes problem with singular sources.
- 6 *Computer Methods in Applied Mechanics and Engineering*, 345:1007–1032, 2019.

- 1 [3] C. J. S. Alves and A. L. Silvestre. On the determination of point-forces on a Stokes system. *Mathematics and Computers*  
2 *in Simulation*, 66:385–397, 2004.
- 3 [4] M. Andrieu and A. El Badia. On an inverse source problem for the heat equation. application to a pollution detection  
4 problem, ii. *Inverse Problems in Science and Engineering*, 23(3):389–412, 2015.
- 5 [5] G. Bastay, T. Johansson, V. A. Kozlov, and D. Lesnic. An alternating method for the stationary Stokes system. *Z. Angew.*  
6 *Math. Mech*, 86:268–280, 2006.
- 7 [6] L. Bourgeois. A mixed formulation of quasi-reversibility to solve the Cauchy problem for Laplace’s equation. *Inverse*  
8 *Problems*, 21:1087–1104, 2005.
- 9 [7] F. Caubet. *Détection d’un Objet Immergé dans un Fluide*. PhD thesis, Université de Pau, 2012.
- 10 [8] R. Chamekh, A. Habbal, M. Kallel, and N. Zemzemi. A Nash game algorithm for the solution of coupled conductivity  
11 identification and data completion in cardiac electrophysiology. *Mathematical Modelling of Natural Phenomena*, 14:Art.  
12 201, 15 pp, 2019.
- 13 [9] A. Cimetière, F. Delvare, and F. Pons. Solution of the Cauchy problem using iterated tikhonov regularization. *Inverse*  
14 *Problems*, 17:553–570, 2001.
- 15 [10] P. Constantin and C. Foias. *Navier-Stokes Equations*. University of Chicago Press, 1988.
- 16 [11] A. El Badia and T. Ha-Duong. An inverse source problem in potential analysis. *Inverse Problem*, 16:651–663, 2000.
- 17 [12] H. A. Eschenauer, V. Kobelev, and A. Schumacher. Bubble method for topology and shape optimization of structures.  
18 *Structural Optimization*, 8:42–51, 1994.
- 19 [13] C. Fabre and G. Lebeau. Unique continuation property of solutions of the stokes equation. *Communications in Partial*  
20 *Differential Equations*, 21:573–596, 1996.
- 21 [14] R. S. Falk and P. B. Monk. Logarithmic convexity for discrete harmonic functions and the approximation of the Cauchy  
22 problem for poisson’s equation. *Mathematics of Computation*, 47:135–149, 1986.
- 23 [15] J. Ferchichi, M. Hassine, and H. Khenous. Detection of point-forces location using topological algorithm in Stokes flows.  
24 *Applied Mathematics and Computation*, 12:7056—7074, 2013.
- 25 [16] P. C. Franzone and E. Magenes. On the inverse potential problem of electrocardiology. *Calcolo*, 16:459–538, 1979.
- 26 [17] A. Habbal and M. Kallel. Neumann-Dirichlet Nash strategies for the solution of elliptic Cauchy problems. *SIAM Journal*  
27 *on Control and Optimization*, 51:4066–4083, 2013.
- 28 [18] A. Habbal, M. Kallel, and M. Ouni. Nash strategies for the inverse inclusion Cauchy-Stokes problem. *Inverse problems*  
29 *and imaging*, 13:827–862, 2019.
- 30 [19] J. Hadamard. *The Cauchy Problem and the Linear Hyperbolic Partial Differential Equations*. Dover, New York, 1953.
- 31 [20] F. Hecht. New development in freefem++. *Journal of Numerical Mathematics*, 20:251–265, 2012.
- 32 [21] E. M. Hussein. The physical and mathematical aspects of inverse problems in radiation detection and applications. *Applied*  
33 *Radiation and Isotopes*, 70(7):1131–1135, 2012.
- 34 [22] T. Johansson and D. Lesnic. Reconstruction of a stationary flow from incomplete boundary data using iterative methods.  
35 *European Journal of Applied Mathematics*, 17:651–663, 2006.
- 36 [23] V. Kozlov, V. Maz’ya, and A. Fomin. An iterative method for solving the Cauchy problems for elliptic equations.  
37 *Computational Mathematics and Mathematical Physics*, 31:45–52, 1991.
- 38 [24] W. Mansouri, T. N. Baranger, H. Ben Ameer, and N. H. Tlatli. Identification of injection and extraction wells from  
39 overspecified boundary data. *Inverse Problems in Science and Engineering*, 25:1091–1111, 2017.
- 40 [25] A. Samuel, I. Horchani, and M. Masmoudi. Crack detection by the topological gradient method. *Control and cybernetics*,  
41 34:81–101, 2005.
- 42 [26] J. Sokolowski and A. Zochowski. On the topological derivative in shape optimization. *SIAM Journal on Control and*  
43 *Optimization*, 37:1251–1272, 1999.
- 44 [27] A. Stephane, A. Ben Abda, and T. N. Baranger. Solving Cauchy problems by minimizing an energy-like functional.  
45 *Inverse problems*, 22:115–133, 2006.
- 46 [28] R. Temam. *Navier-Stokes Equations: Theory and Numerical Analysis*. American Mathematical Society, 2001.